EUROPEAN COMMISSION
5th EURATOM FRAMEWORK PROGRAMME 1998-2002
KEY ACTION : NUCLEAR FISSION

HTR-E

High-Temperature Reactor Components and Systems

CONTRACT N°
FIKI-CT-2001-00177

D19 Recuperator: Validation tests on Heatric Mock up

F. PRA (CEA / FRANCE)

Dissemination level: RE
Document N°: HTR-E-05/11-D-2-3-3
Status: Final
Deliverable n°19

Direction de la recherche technologique
Laboratoire d'innovation pour les technologies
des énergies nouvelles et les nanomatériaux
Département des systèmes pour les énergies nouvelles
Service GREThE
LETH

Rapport technique DSEN/DR/2005/094

"HTR-E – D19 RECUPERATOR:
VALIDATION TESTS ON HEATRIC MOCK UP"

Auteur : Franck PRA

Référence du contrat	
Référence PRODEM	05-00934-1
Nature du rapport	Avancement
Confidentialité	Les informations contenues dans le présent document sont la propriété des contractants. Il ne peut être reproduit ou transmis à des tiers sans l'autorisation expresse des contractants.

	Rédacteur	Vérificateur	Approbateur
Nom	***F.PRA***	***P.TOCHON***	***P.MERCIER***
Fonction	Chef de projet	Responsable Technique	Chef de Laboratoire
Signature			
Date	5/12/2005	8/12/2005	12/12/2005

LISTE DE DIFFUSION

Rapport complet à :

PARTNENAIRES	D.BESSON (Framatome ANP Lyon)	5 ex.
	C.MAUGET (Framatome ANP Lyon)	1 ex.
	S.DEWSON (HEATRIC U.K.)	2 ex.
	W.LEVY (HEATRIC France)	1 ex.
	J.FOKKENS (NRG NDL)	1 ex.
	L.CINOTTI (ANSALDO Italie)	1 ex.
DEN/DDIN/SF	F.CARRE	1 ex.
	Ph.BILLOT	1 ex.
	B.LINET	1 ex.
DEN/CAD/DER/STR	A.BERJON	1 ex
DSEN/DIR	Chef de Département et son adjoint	1 ex.
	Correspondant Programme du thème de la note	1 ex.
DSEN/GREThE	C. MARVILLET	1 ex.
	P.MERCIER	1 ex.
	P.TOCHON	1 ex.
	F.PRA	1 ex.
	P.CLEMENT	1 ex.
	Archivage	Original + 1 ex.

Page de garde + résumé + Liste de diffusion à :

Chefs des autres services du DSEN
Chefs des laboratoires du service

Page de garde + résumé + Liste de diffusion + Lettre d’envoi à :

Ingénieur Qualité
Bureau financier (Ventes)

Résumé

Résumé : Ce document présente le livrable 19 du WP 'Recuperator' du projet HTR-E. Le rapport présente les résultats thermo hydrauliques et thermo mécaniques de la maquette HEATRIC testée sur la boucle CLAIRE du GREThE.

Abstract:
This document presents the deliverable 19 of the WP 'Recuperator' of the HTR-E project. Results of thermal, hydraulic and thermo mechanical tests carried out on a HEATRIC mock up are presented. The heat exchanger was tested on GREThE CLAIRE loop

TABLE OF CONTENTS

INTRODUCTION

Within the HTR-E program, some recuperators have to be tested on a test rig of the GREThE. Experimental tests were carried out on a mock up designed by HEATRIC. These tests were done on CLAIRE loop located at CEA research centre at GRENOBLE.

To carry out thermal and hydraulic tests in steady and transient conditions, GREThE has to modify one of its test rigs to fit to recuperator specification.

1. DESIGN OF THE MOCK UP

The table 1 reminds the typical thermal and hydraulic steady state working conditions. The values are extracted from “HTR-E-Recuperator, specifications of typical operating conditions for HTR” written by Framatome ANP [1].

Name of parameter	Value
Thermal capacity	635 MWth
Thermal effectiveness	0.95
Helium parameters on low pressure side	
flow rate	316 kg/s
inlet temperature	510 °C
outlet temperature	125 °C
inlet pressure	2.63 MPa
pressure losses	no more than around 0.03 MPa
Helium parameters on high pressure side	
flow rate	313 kg/s
inlet temperature	105 °C
outlet temperature	490 °C
inlet pressure	7.07 MPa
pressure losses	not more than around 0.07 Mpa (instead of 0.03 Mpa in Framatome’s report)
ΔP between the high and low pressure sides	4.5 MPa

Table 1 : GT-MHR typical steady state working conditions

In accidental cases, some potential transients have been identified. For the recuperator, the most severe case generates high temperature variations. On low pressure side, the temperature at the inlet of the recuperator may decrease from 510 to 180°C within 5 seconds and it may reach again 510°C within 120 seconds.

According to these specifications, HEATRIC has designed a whole recuperator. Based on this design, a mock up was manufactured to fit to CLAIRE loop specifications (especially mass flow rate and pressure working conditions).

1.1 MAIN SPECIFICATIONS OF THE MOCK UP

The heat exchanger is realised with a stack of plates alternatively hot and cold ones. A scheme of the plates is given in figure 2 showing 2 main areas:

- Pink area: thermal active part of the plate
- Blue area: fluid distribution part

The thermal active area is made of wavy channels (figure 1) whereas fluids distribution channels are straight ones.

Figure 1 : Example of wavy corrugations

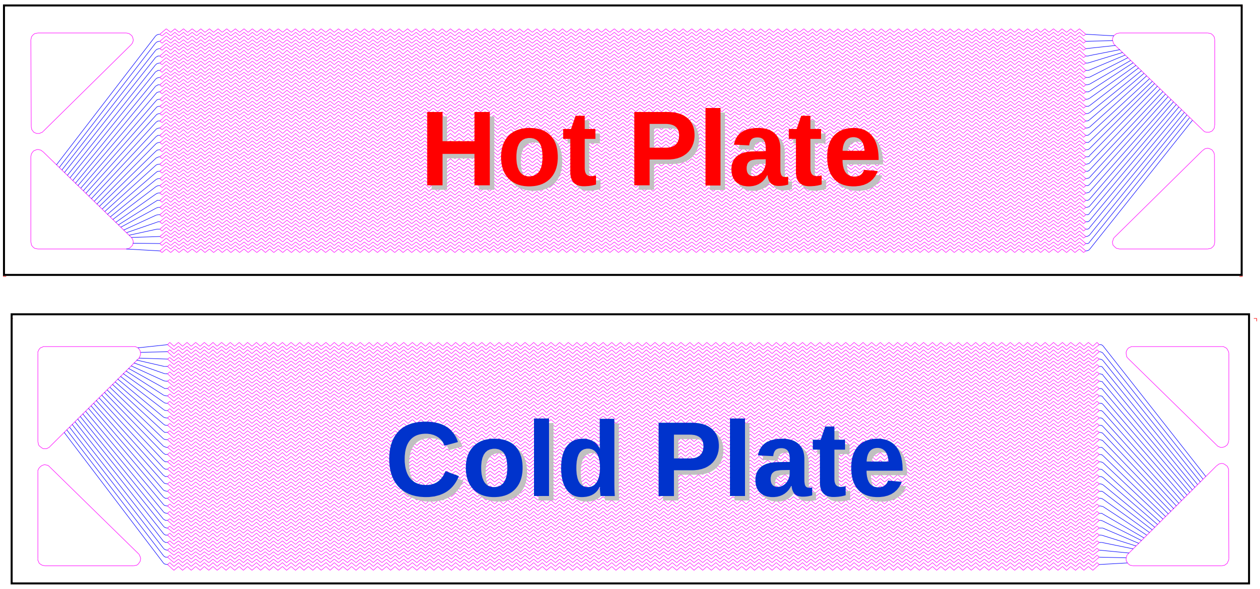

Figure 2 : Scheme of the plates

Once the plates are stacked together and diffusion bonded, it gives raise to the whole heat exchanger whose main dimensions are given on figure 3.

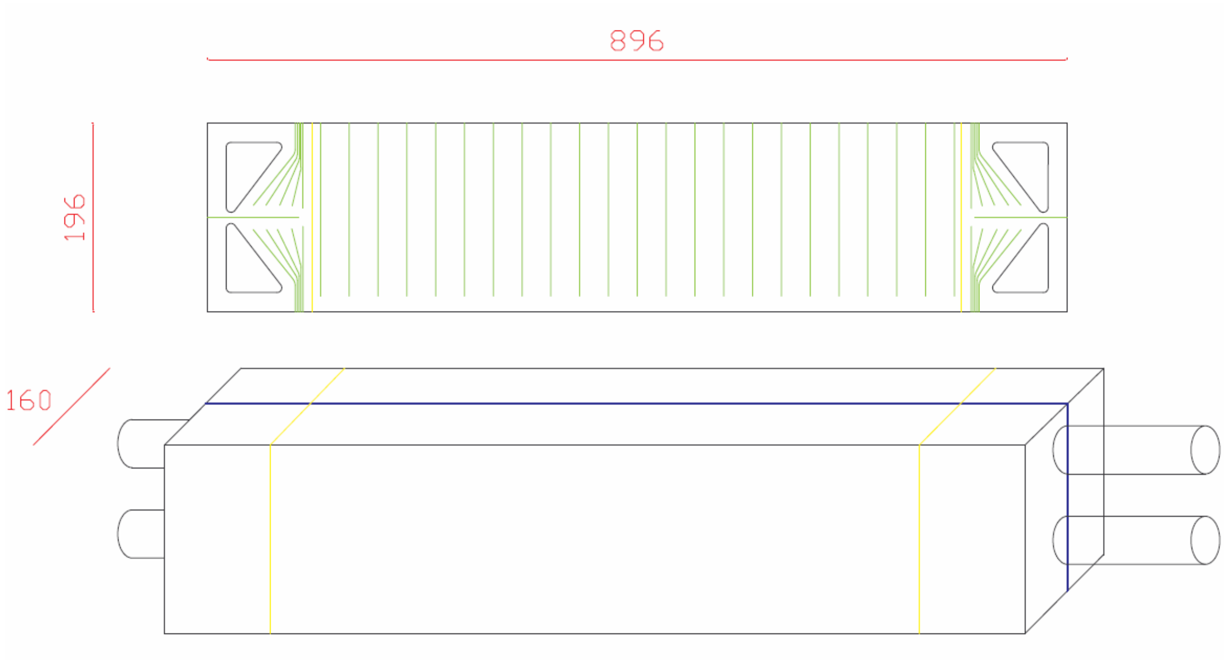

Figure 3 : Main dimensions of the HEATRIC mock up

In the middle of the mock up, an instrumentation plate was slid between a hot and a cold plate to realize temperature mapping.

Figure 4 : Photo of the HEATRIC mock up

More detailed specifications are given in table 2.

Side		A	B
	units		
No Plates	-	50.0	50.0
Surface area	m^2	11.958	
dh	m	0.001	0.001
active length	m	0.672	0.672
no lines/plate	-	62.0	62.0
free flow area	m^2	0.00361	0.00361

Table 2 : Geometrical data given by HEATRIC

Channels are identical on both sides of the heat exchanger.

1.2 INSTRUMENTATION

1.2.1 Local instrumentation on the mock up

The mock up is locally instrumented with:

- 25 thermocouples inside the HX (9 in the active part and 16 near in the distribution areas)
- Strain gauges (outside plate of the HX)

Thermocouples located in the active part of the heat exchanger can be moved along the width of the heat exchanger so that it is possible to realize a temperature mapping. These thermocouples can used to estimate a possible flow mal distribution between channels of one plate.

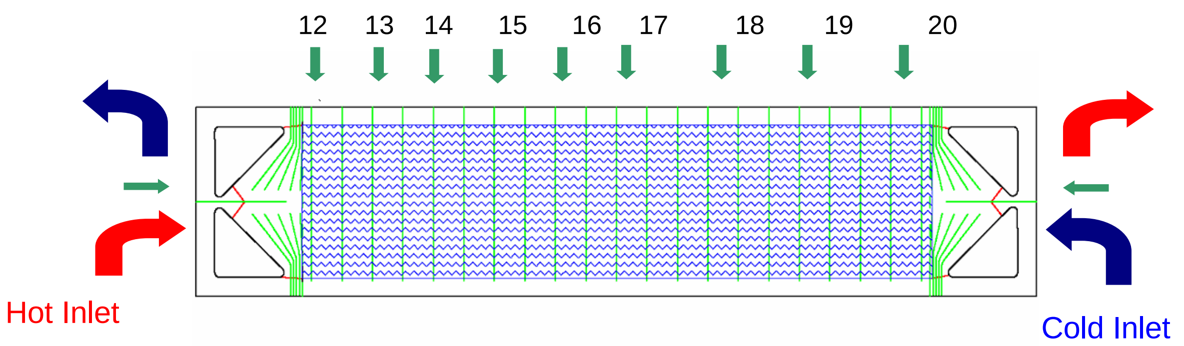

Figure 5 : Internal thermocouples location

The core is externally instrumented with local strain gauges so that it is possible to estimate stresses generated by thermal shocks during temperature transient. As it is not possible to put such devices inside the core, the gauges are supposed to give lower stresses than those generated inside; nevertheless they can give important information.

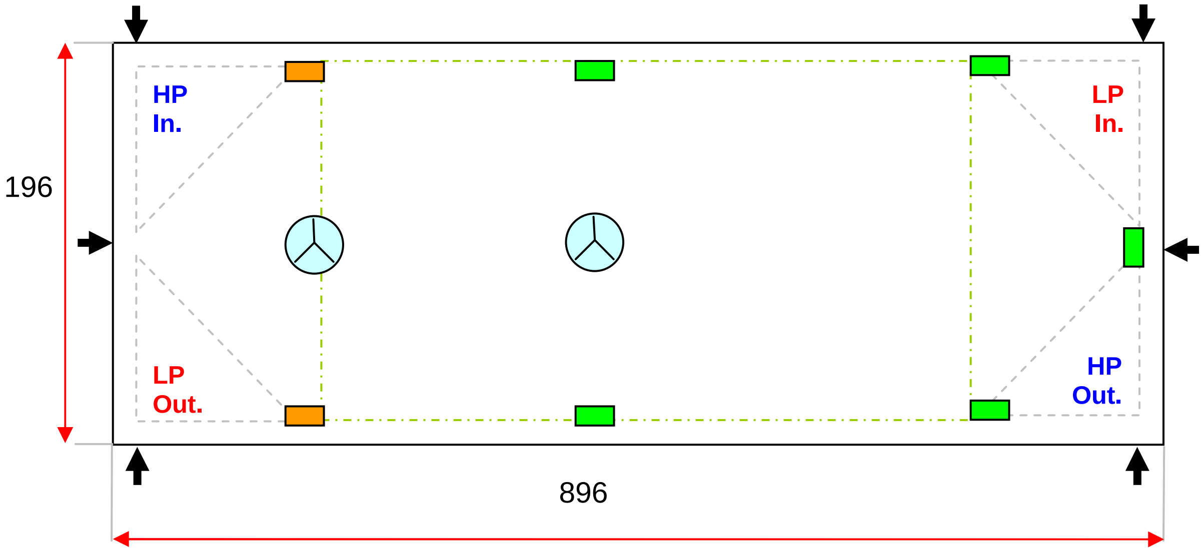

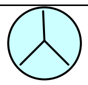	Tri dimensional gauge
	Unidirectional welded gauge
	Unidirectional glued gauge
	Global displacement sensors

Figure 6 : Strain gauges location

1.2.2 CLAIRE loop and global instrumentation

CLAIRE is an air open loop and the heat exchanger is fed by a compressor on both sides. It includes 2 different circuits:

- A hot one
- A cold one

Depending on the heat duty one or two compressors are used. A tank is fed by compressor(s) and is equipped with regulation valves so that the flow rate remains steady.

The loop is designed to test significant size of heat exchangers. So the maximum mass flow rate is limited to 0.2 kg/s on both side and the maximum operating pressure at the inlet of the heat exchanger is 6 bars.

Table 3 gives the nominal operating conditions of CLAIRE loop.

	Hot side (600)	Cold side (500)
Mass flow rate (kg/s)	0.04 <M<0.2	
Inlet HX temperature (°C)	510 (up to 550)	105
Inlet HX pressure (Bar)	~6	~6
Allowed HX pressure drop (bar)	~2	

Table 3 : Nominal working conditions

To estimate general performances of the mock up, the loop is equipped with flow meters, thermocouples and pressure sensors at the inlet and the outlet of the mock up. Global displacement sensors were also used on the mock up as shown on figure 6.

A scheme of the loop with global instrumentation is given on Figure 7.

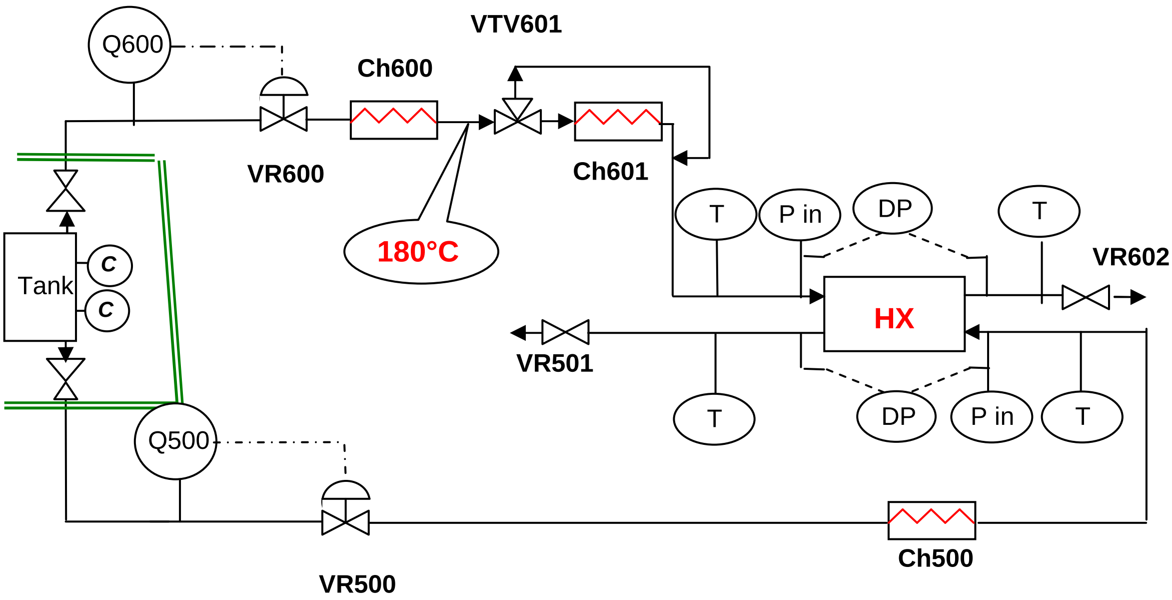

Figure 7 : Scheme of CLAIRE loop with global instrumentation

2. TESTS AND PERFORMANCES IN STEADY STATE

To characterize the heat exchanger in steady state condition, it is necessary to determine hydraulic and thermal performances. The final objective is to check whether predicted performances are reached or not.

2.1 HYDRAULIC PERFORMANCES

The hydraulic friction law could be expressed in the following way:

$$f = a\,Re^{-b}$$

With:

f : Fanning number
Re : Reynolds number

$$Re = \frac{\rho \times u \times dh}{\mu}$$

ρ : Fluid density (kg/m^3)
u : Fluid bulk velocity (m/s)
μ : Dynamic viscosity (Pa.s)
dh : Hydraulic diameter (m) (data provided by Heatric cf table 2)

To determine the hydraulic friction law in the heat exchanger, global pressure drops are measured between the inlet and the outlet of the core. Pressure drops and Fanning factor are linked by the following expression:

$$\Delta P = 4f \times \frac{l}{dh} \times \frac{1}{2}\rho u^2$$

With

l : thermal active length of the heat exchanger

The measured pressure drops integrate several terms such as inlet effects, core friction and outlet effects so it is necessary to make corrections to estimate the pressure drops generated only by the thermal active area. Figure 8 shows singularities which have been taken into account to correct the pressure drops.

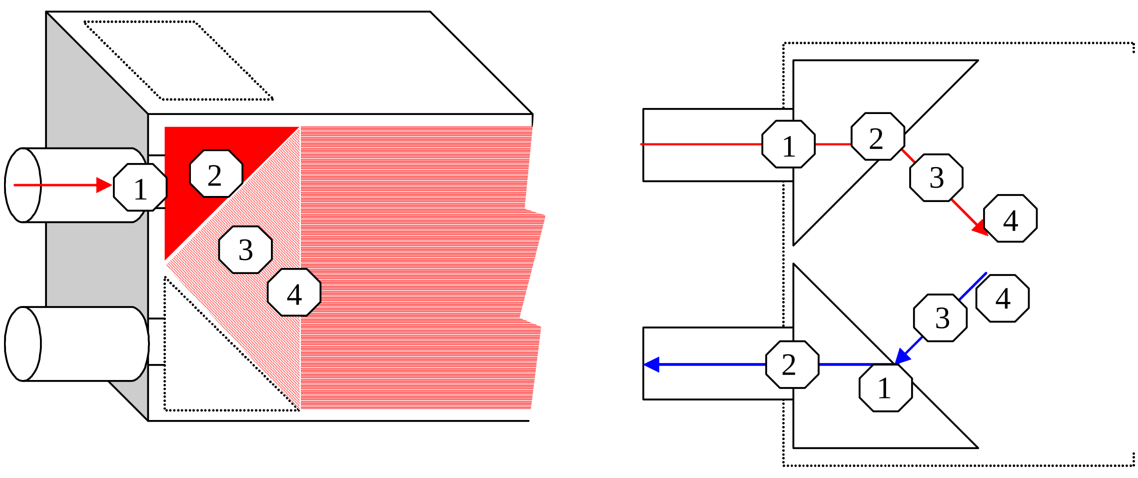

Figure 8 : Considered singularities

1 : Sudden widening (between inlet pipe and header)
2 : Sudden narrowing (between header and channel)
3 : Core friction in distributing channels
4 : Direction change between distributing channels and thermal active channels

Hydraulic tests were performed at ambient temperature to avoid needed corrections on fluid properties. Figure 9 shows the friction coefficient versus Reynolds number.

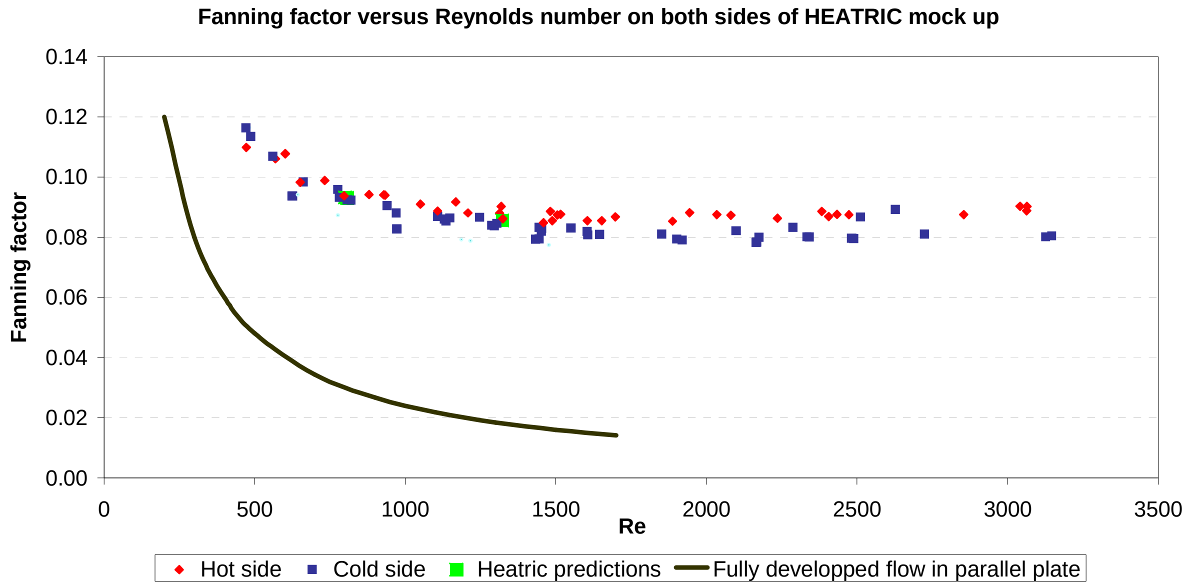

Figure 9 : Experimental hydraulic results

Calculations of Fanning factor issued from experimental tests lead to a good agreement between experimental tests and Heatric predictions. Figure 9 shows a slight difference between hot and cold side especially at high Reynolds numbers. It could be explained by sensors uncertainties but the inversion of sensors between hot and cold sides did not lead to significant variations.
Regarding to literature [3], such corrugated channels are known to generate secondary flows even in laminar flow giving raise to higher Fanning factor than one in parallel plates. The ratio of Fanning coefficients between such geometries is strongly affected by the geometrical characteristic of the corrugation (angle, wavelength). The confidentiality of the exact shape of the waves does not allow knowing the real parameters of the waves but the experimental measurements tend to confirm general information of the literature:

- the transition to unsteady flow occurs at lower Reynolds number i.e. around 1200
- at higher Reynolds number, the friction factor is nearly independent of Reynolds number (at least in the experimental Reynolds range).

2.2 THERMAL PERFORMANCES

Thermal tests are realised to determine local heat exchange coefficients and to check Heatric prediction. As for hydraulic tests, Heatric has provided predictive results for 3 different mass flow rates.

The local heat exchange coefficient is calculated in the following way:

- From global measurements between the inlet and the outlet of the exchanger, global heat exchange coefficient is determined.

$$U = \frac{\left(Q_{hot\ side} + Q_{cold\ side}\right)/2}{A\ LMTD} \quad (1)$$

with :
$Q_{cold,\ hot}$: heat transfer rate in the heat exchanger on hot and cold side (W)

$$Q_{c,h} = (mCp)_{c,h}\left|\left(T_i - T_o\right)_{c,h}\right|$$

m : mass flow rate (kg/s)
Cp : specific heat (J/kg/℃)
T : temperature (℃)
i : inlet
o : outlet

A : Developed heat transfer surface area (m^2) (data given by HEATRIC cf table 2)
LMTD : logarithmic mean temperature difference (℃)

Since working conditions on both sides of heat exchanger are quite similar and since hot and cold geometries are the same, it is possible to estimate local heat exchange coefficient for an average Reynolds number. Therefore, from (1), local heat exchange coefficients are determined as follow:

$$\frac{1}{\alpha} = \frac{1}{2}\left(\frac{1}{U} - \frac{e}{\lambda}\frac{A}{A_{proj}}\right) \quad (2)$$

e : Plate thickness (m) (~ 0.4 mm)
λ : Thermal conductivity of metal (~ 16 W/m/K)
A_{proj} : Projected heat transfer surface area (m^2)

From (2), thermal behaviour of the heat exchanger is expressed as a non-dimensional thermal law using Nusselt number for each experimental Reynolds number.

$$Nu = \frac{\alpha \; Dh}{\lambda_{fluid}}$$

with
λ_{fluid} : mean thermal conductivity of cold and hot fluids between the inlet and the outlet
Pr : mean Prandtl number of cold and hot fluids between the inlet and the outlet

$$Pr = \frac{\mu \; Cp}{\lambda}$$

For each experimental point, Nusselt number is calculated on hot and cold sides and the average value is plotted as a function of $Nu / Pr^{1/3}$ versus average Reynolds number.

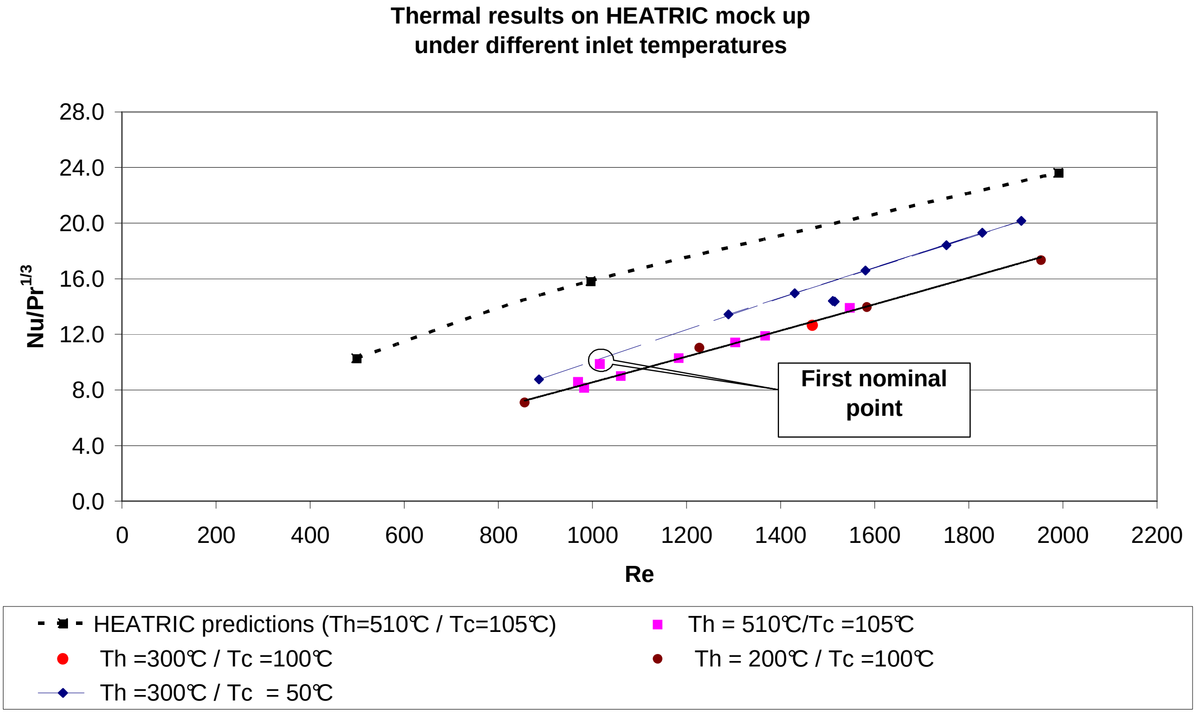

Figure 10 : Experimental thermal results

The initial aim of thermal tests was to carry out experimental tests with respect to GT-MHR inlet working temperatures and desired effectiveness. Nominal mass flow rate was defined in order to keep GT-MHR working Reynolds number that leads to a nominal mass flow rate of 0.1 kg/s. It was decided to realize tests between half and twice the nominal mass flow rate. Therefore, Heatric provided three theoretical calculations, at nominal working temperatures, which are plotted on figure 10 (black dotted line).

Figure 10 leads to the following remarks:

- Considering the experimental tests carried out at nominal inlet temperatures (i.e. T hot inlet =510℃ and T cold inlet =105℃), a quite significant discrepancy is obtained compared to Heatric prediction: factor 1.6 between experimental results and predictions at nominal mass flow rate. In other way, the measured outlet temperatures are different of around 10℃ (over a temperature change of 395℃ between the inlet and outlet of the HX) compared to predicted temperatures.

- From these results, further tests were carried out at different inlet temperatures to investigate undesired effects of wall conduction. The lowest temperature difference between hot and cold inlet (i.e. $T_{h,in}$ = 200℃ and $T_{c,in}$ = 100℃) gave the same results than the previous ones : brown points are aligned with pink ones on figure 10.

- Experimental tests carried out with $T_{h,in}$ = 300℃ and $T_{c,in}$ =50℃ lead to highest performances than any other working conditions without obvious reasons. For this first test campaign, it was decided to start the loop at moderated temperatures (so 300℃ on hot side) giving raise to the blue dashed line on figure 10. These tests were followed by a point "first nominal point" on figure 10 which is aligned with points at 300℃. After this first raising to 510℃, all the experimental results were a little lower and whatever the inlet temperatures are. So it is possible that thermocouples located in hottest areas (hot side inlet and cold side outlet of the HX) have been affected in the same way by the temperature increase leading to this difference between first tests and further ones. Nevertheless, this assumption does not explain the discrepancy between experimental results and predicted ones.

- Whatever the inlet temperatures are, the experimental thermal laws lead to unexpected results in term of correlation. Usually, thermal laws are expressed in following way :

$$Nu = a\,Re^{b}\,Pr^{c}$$

Where coefficients *a* and *b* are function of geometry and *c* varies between 0.3 and 0.4 generally depending on the fluid “function” (cooling or heating). Depending on the Reynolds number, b coefficient varies between 0.4 and 0.8. The experimental tests lead to b coefficient, which is slightly over than one whereas it should be around 0.6-0.8 for this geometry. Therefore, it is necessary to try understanding the reasons why thermal performances become much higher when experimental Reynolds numbers are increased and why there is such a discrepancy between experimental results and predictions.

Two main explanations are possible:

- Flow mal distribution between channels generating a loss of efficiency
- Longitudinal wall conduction: Instead of transferring completely available heat from hot side to cold side, a part of heat flux is transferred along the plate itself between the inlet and the outlet of the HX. This phenomenon tends to flatten the wall temperature profile, which directly reduces the efficiency of the heat exchanger.

2.2.1 Flow mal distribution

Since the internal thermal active part of the HX is instrumented with thermocouples, it is possible to realise a temperature mapping along the width of the plate giving information about flow distribution within one plate. Depending on measured temperatures, it is also possible to get information about distribution between plates.

Figure 11 shows a temperature mapping of the HX carried out at nominal point.

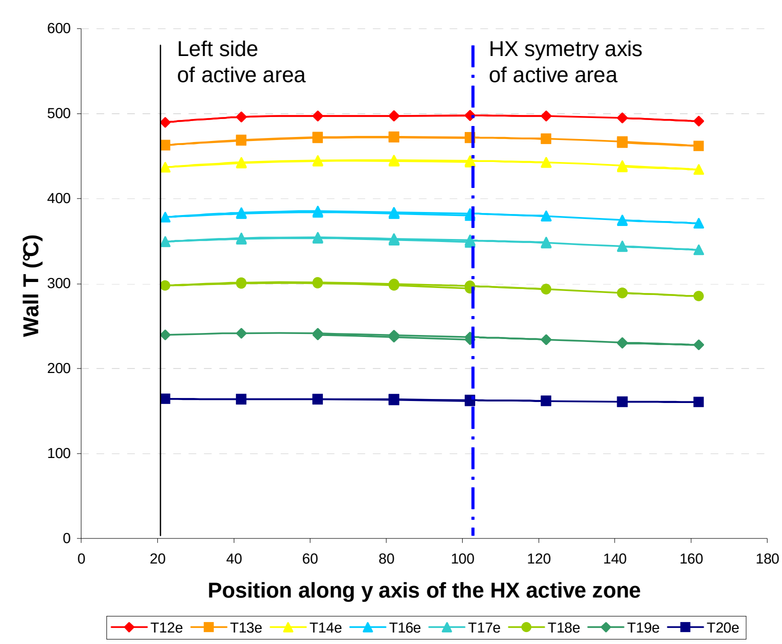

Max DT (°C)
8.3
10.7
10.9
14.4
14.5
16.3
14
3.7

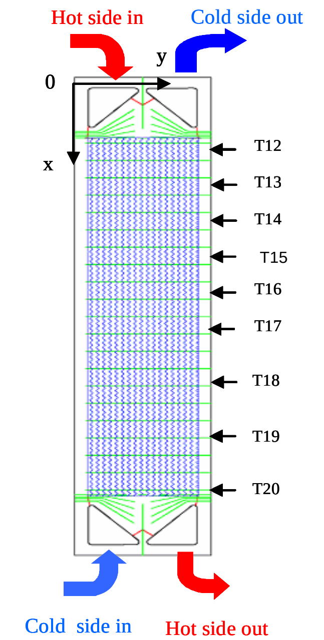

Figure 11 : Experimental thermal mapping

Max DT stands for the maximum temperature deviation for one thermocouple along y-axis.

The temperature mapping shows:

- For each thermocouple, the temperature profile is symmetrical with respect to HX symmetry axis: apparently, the flow distribution is the same on both sides of the symmetry axis.
- Temperature profiles are quite flat, which tends to show there is no flow mal distribution between the channels within the same plate (width effect).

These experimental measurements do not match with numerical simulations, which tend to conclude to mal distribution between channels of one plate generated by the cross flow distributing areas. For more information concerning simulations, refer to Thermal and Mechanical Analyses for Heatric Mock up, deliverable 15 of the HTR-E WP2.

If experimental measurements conclude apparently to a correct fluid distribution between channels of the same plate, it does not mean that the plates are fed in the same way from one to another (height effect). Nevertheless, it can be checked by using also the internal temperature measurements.

Since the geometry of the channels is identical on both sides of heat exchanger and the experimental flow rate between hot and cold sides are identical, the theoretical wall temperature can be estimated for each desired position. These theoretical temperatures can be compared to experimental temperatures along the symmetry axis of the heat exchanger.

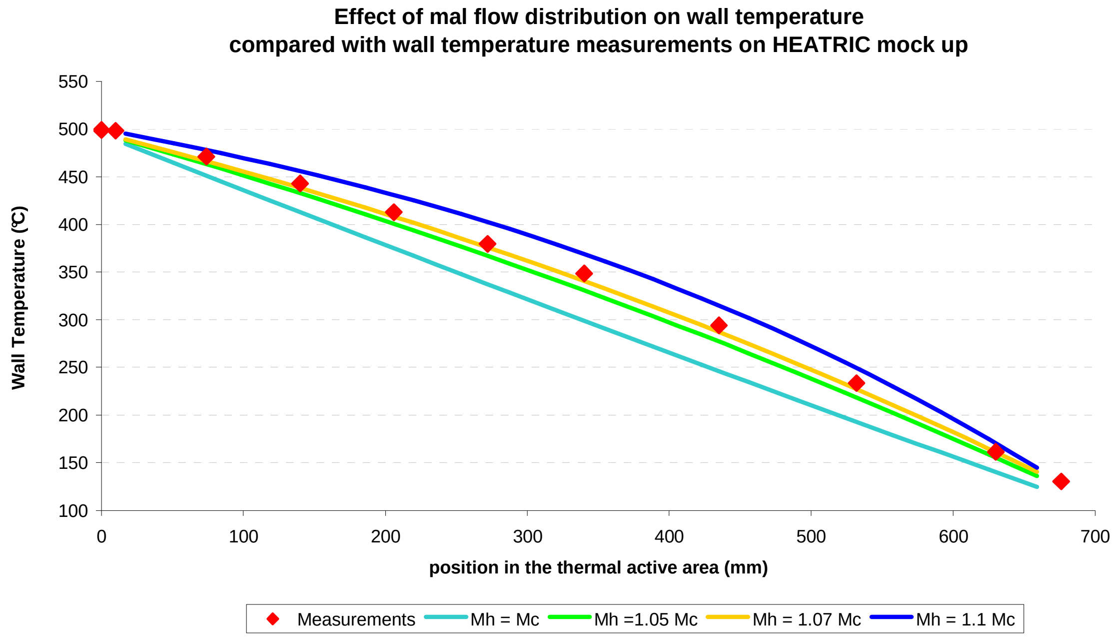

Figure 12 : Temperature profile along symmetry axis

As shown on figure 12, it is necessary to increase hot mass flow rate (or decrease cold mass flow rate) compared to cold one to fit with temperature measurements. The optimal results seem to be obtained when the hot mass flow rate is multiplied by 1.07. So, at equal global mass flow rate between hot and cold sides, an increase of hot local mass flow rate in the central channels mean a decrease in other channels. This eventual mal distribution could explain the discrepancy between experimental and predicted results (or at least it may be one of the reasons).
Since the inlet channels are directly in front of the inlet pipe, a jet effect at the inlet can affect the flow distribution. On hot side as the air density is lower than the one of the cold side, the inlet velocity is higher leading to different flow distribution between channels.

2.2.2 Longitudinal wall conduction

To study the effect of longitudinal wall conduction on the heat exchanger efficiency, a method proposed by Kroeger [3] is used for counter current heat exchanger.
The method allows determining the efficiency of heat exchanger affected by axial conduction. To do that, a longitudinal conduction parameter is defined:

$$\lambda = \frac{k_w \times A_k}{L \times C_{\min}}$$

With

k_w : Wall conductivity (W/m/K)
A_k : Wall frontal area (m²)
L : Length of the active area (m)
$C_{\min}$: Minimum fluid capacity between hot and cold side (W/°C)

From this parameter, the real effectiveness is expressed as follows:

$$\varepsilon = 1 - \frac{1}{1 + NTU \times (1 + \lambda \times \Phi)/(1 + \lambda \times NTU)}$$

With :

NTU : Number of Thermal Units, UA/C_{min}

$$\Phi = \left(\frac{\lambda \times NTU}{1 + \lambda \times NTU} \right)^{1/2}$$ Valid for $NTU \geq 3$.

Applying this method, it leads to a real effectiveness of 97.1 % instead of 97.6% so longitudinal wall conduction may contribute to difference between measurements and prediction but it cannot be considered as the main reason: in term of temperature, it generates 2°C difference on *LMTD*, so instead of getting *LMTD* = 10°C we get *LMTD* = 12°C.

For comparison, the Kroeger method was checked by using a finite elements method, which led to the same conclusion.

2.2.3 Conclusion on thermal tests in steady state

With respect to GT-MHR working temperatures, experiments were carried out on CLAIRE loop with air. Mass flow rate on hot and cold sides were varied as much as possible to estimate thermal behaviour in Reynolds numbers range around nominal Reynolds number of GT-MHR. At first look, an important discrepancy is obtained between experimental results and predicted one, since factor 1.6 was obtained on Nusselt number at nominal mass flow rate. Further investigation may explain this discrepancy without having doubts about thermal law of the corrugated channels. From initial prediction given by HEATRIC at nominal point, the effectiveness was supposed to be around 97.6 %. Three main corrections could explain the experimental effectiveness equals to 95.3% (+/- 0.3 % with 1℃ of accuracy on temperature measurements):

- An adjustment of air physical properties generates a decrease of effectiveness of 0.8 %
- Adding an effect of longitudinal wall conduction leads to a decrease of effectiveness of 0.5 %
- Assuming a flow mal distribution between plates can easily generate a loss of effectiveness around 1%.

Concerning the last point, sensitivity study was done considering a parabolic mass flow rate profile distribution on hot side and a flat one on cold side. On hot side, the profile was adjusted so that the maximum mass flow rate was in front of the inlet pipe and was 7% over the average hot mass flow rate. The global effectiveness is then decreased by 0.9% compared to expected result.

So by adding the three effects, the experimental effectiveness can be justified. Moreover, it must be kept in mind that the heat exchanger fulfils the specification in the way that 95% effectiveness is reached as in GT-MHR specification.
In addition to these conclusions, if the discrepancy was linked to an error on thermal law in corrugated channels, the experimental effectiveness should not increase when mass flow rates are increased.
So to go further in these investigations, it would be worth modifying the inlet pipes to avoid (or decrease) this jet effect which seems to occur more especially on hot side since the inlet velocity is higher than one on cold side. For GT-MHR application, HEATRIC did not propose the same alimentation of the channels and therefore no jet effect would occur at the inlet.

3. TESTS AND PERFORMANCES IN TRANSIENT CONDITIONS

The document “HTR-E-Recuperator, specifications of typical operating conditions for HTR” written by Framatome ANP [1] specifies some transient conditions which could occur during reactor life. Depending on the event, the magnitude of the transient may be more or less severe for the recuperator. So it was decided in agreement with all the partners to study the most severe transient. This case corresponds to a loss of offsite power with turbo machine trip. Since it was not possible to generate all parameters variations (temperature, pressure, mass flow rate), it was decided to focus the study on temperature variations effects and to repeat these temperature variations as much as possible.
Therefore, the same GT-MHR temperature variations were applied on the mock up with the following data:

	Specification of inlet temperature on hot side
Cold shock	From 510 ℃ to 180 ℃ within 5 seconds
Hot shock	From 180℃ to 510℃ within 120 seconds

3.1 EXPERIMENTAL PROCEDURE

Figure 13 shows how the temperature transients are generated on CLAIRE loop.

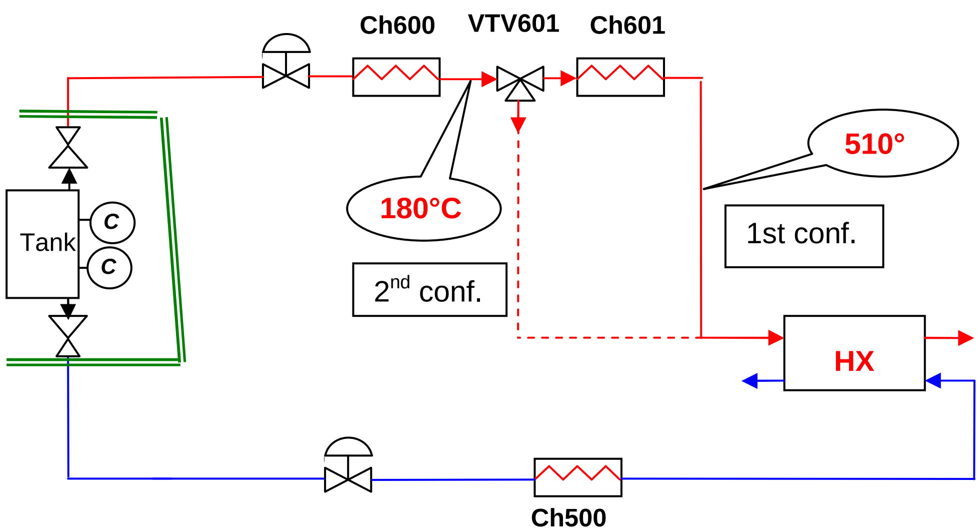

Figure 13 : CLAIRE loop in transient configuration

As the hot side of the loop is equipped with 2 heaters (heater 600 and heater 601) it is possible to bypass the second one (heater 601) to vary quickly the inlet temperature of the heat exchanger. The outlet temperatures of heaters 600 and 601 are regulated at 180℃ and at 510℃ respectively. In first configuration, the HX inlet temperature is equal to 510℃, if the VTV 601 valve is commutated in 2nd configuration, the HX inlet temperature decreases immediately from 510℃ to 180℃, generating the col d shock. In the other way, the hot shock is generated by commutating the valve from the second configuration to the first one. The temperature variation is not immediate since it is function of the performances of heater 601, so it requires around 4 minutes to reach 510℃ at t he inlet of the heat exchanger.

The objective of such transient tests was to study the thermo mechanical behaviour of the HEATRIC heat exchanger and eventually to determine the required number of cycles to generate a failure in the heat exchanger. So to carry out this task, it was decided to repeat always the same thermal load. To be in most damaging configuration, once a shock was generated it was necessary to delay the following one so that HX inside temperatures has time to evolve. Since the heat exchanger has a certain thermal inertia, no delay would mean no temperature variations inside the core and therefore no damage. This delay between two shocks was experimentally defined as shown on figures 14 and 15.

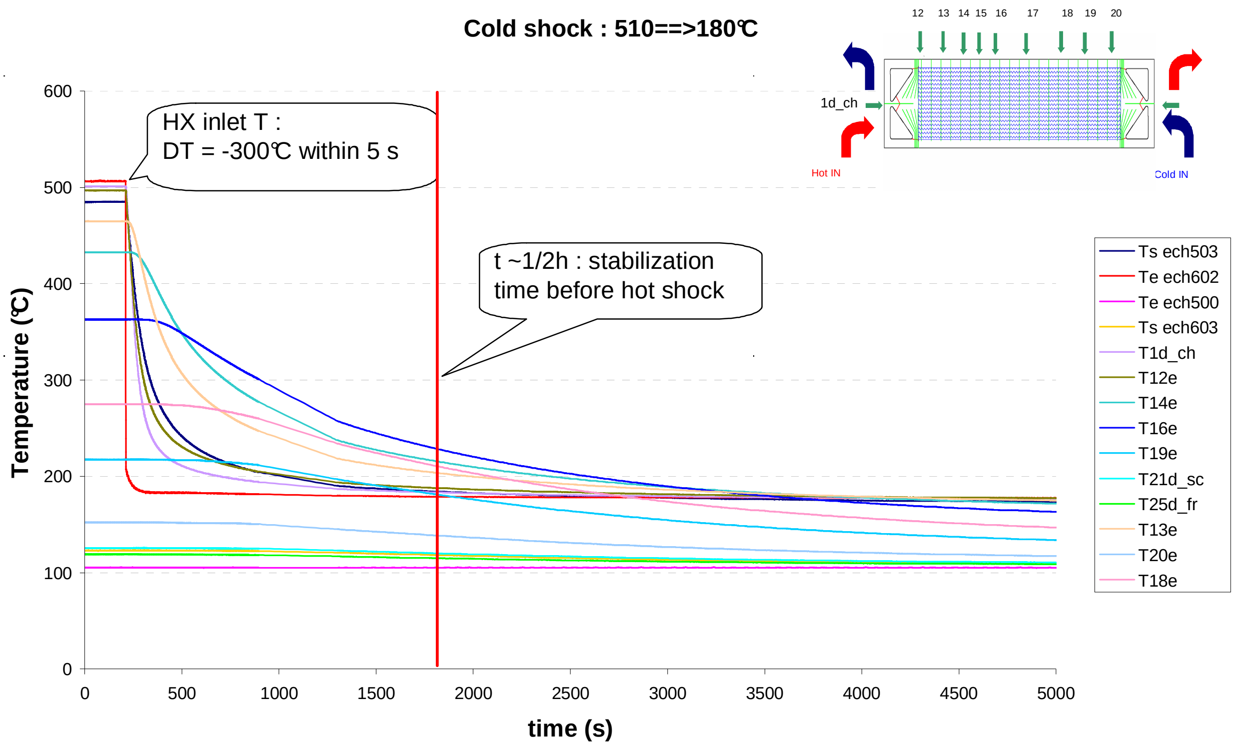

Figure 14 : Typical cold shock on HEATRIC mock up

From temperature variations inside the mock up, it was decided to wait 1/2 hour before generating the hot shock so that the inside temperatures have decreased significantly.

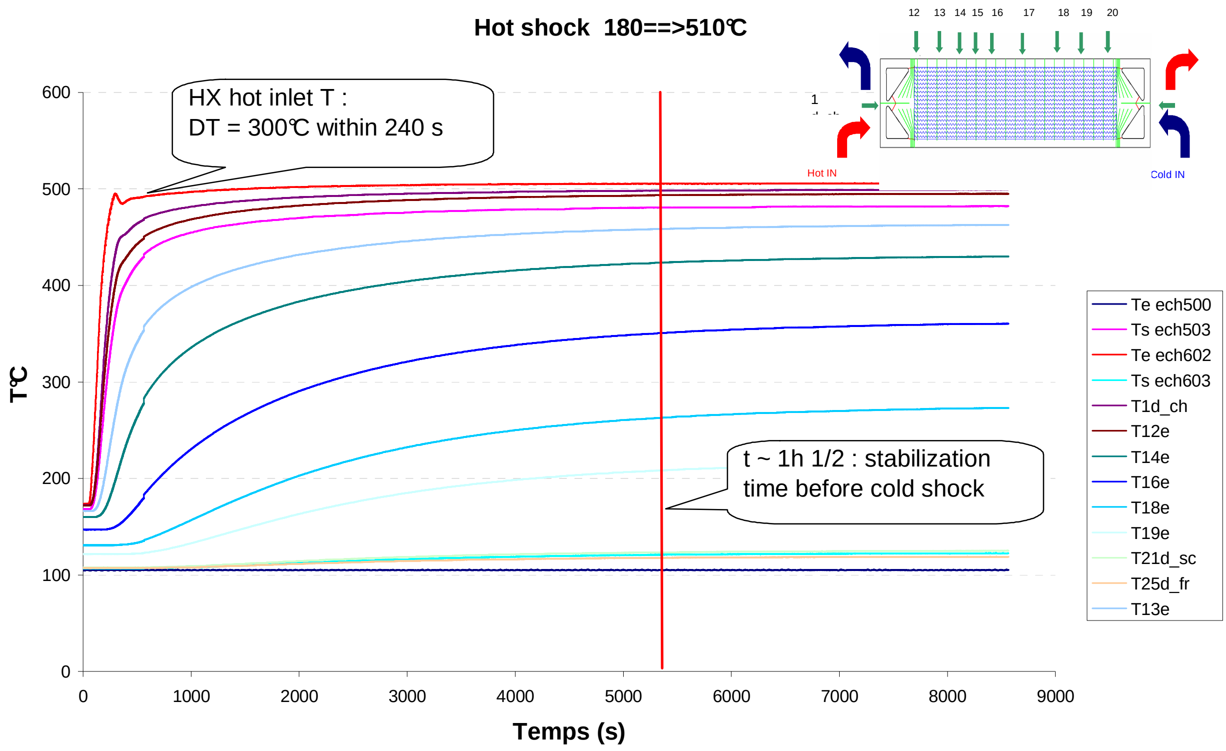

Figure 15 : Typical hot shock on HEATRIC mock up

A longer stabilization time was experimentally required to be back to almost steady temperatures then 1 h 30 was adopted before the next cold shock.

Finally, once these delays were defined, thermal loads were applied every day as shown on figure 16.

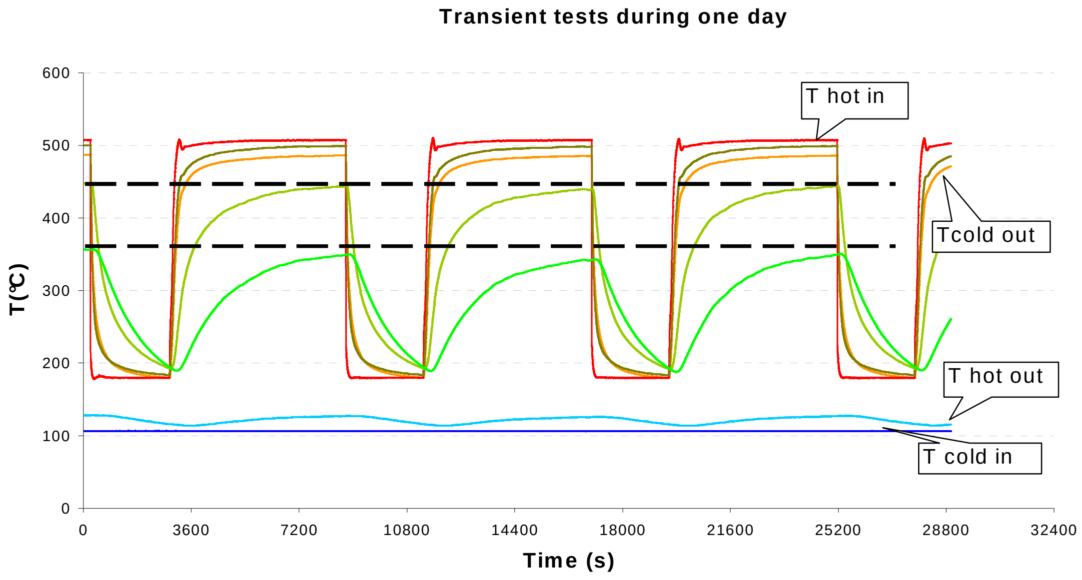

Figure 16 : typical series of thermal shocks applied daily

As shown by black dotted lines, generated shocks were quite similar from one to another. Since no shock was applied during the night, the heat exchanger has time to be back to its nominal state before every series of shocks assuring the similarity of the shocks day per day. Every Monday, a helium test was applied on the mock up to check eventual leaks between hot and cold sides.

3.2 MAIN RESULTS UNDER TRANSIENT CONDITIONS

As said in paragraph 2.2 “instrumentation”, the heat exchanger was instrumented with strain gauges to study its thermal behaviour. The French Welding Institute, which is used to such experiments, realized this task. Their test report is given in annex 1.

From strain measurements on different locations outside of the core, stresses are calculated. Strains and stresses evolutions are studied as a function of time.
Main conclusions of their report are the following ones:

- Initial measurements of strain or stress (in steady state before a cold or a hot shock) are not constant in time: these variations tend to show a modification of the behaviour of the heat exchanger.
- Strains and stresses variations are more important on gauges located on same side than hot inlet and furthermore for the gauge close to the inlet.
- During a thermal shock, when the hot side of the heat exchanger is in a compressive state, the central part is in tensile state and vice versa.
- Stress evolution as a function of the time near the hot inlet is a sign of important plasticity in this area and it may be the sign of a fatigue defect: This tendency is found in literature, submitted to a cyclic stress, mean and peak stresses tend to vary versus time. These variations are explained by local plastic and creep strain accumulation.

- Compared to literature, under a nominal stress of 375 MPa (stress amplitude generated on the mock up) the fatigue life of a SS 304 notched plate is estimated between 150 and 350 cycles at 600℃.

Nevertheless, after 100 cycles realised on Heatric mock up no leak was detected under helium tests and global thermal performances remain the same along the test campaign.

Compared to NRG simulations [4], following remarks can be done:

- A cool down transient generates compressive stresses near the hot inlet whereas a hot shock leads to tensile stresses in the same area.

- Stresses levels are the same order of magnitude for a cold or a hot shock.

- NRG estimated local stresses for different positions as shown below. Concerning points A, B and F "calculated results should be viewed with caution" since these positions are located at geometric discontinuities. Unfortunately, strain gage 1 is supposed to be located on point A, therefore it is difficult to make direct comparisons.

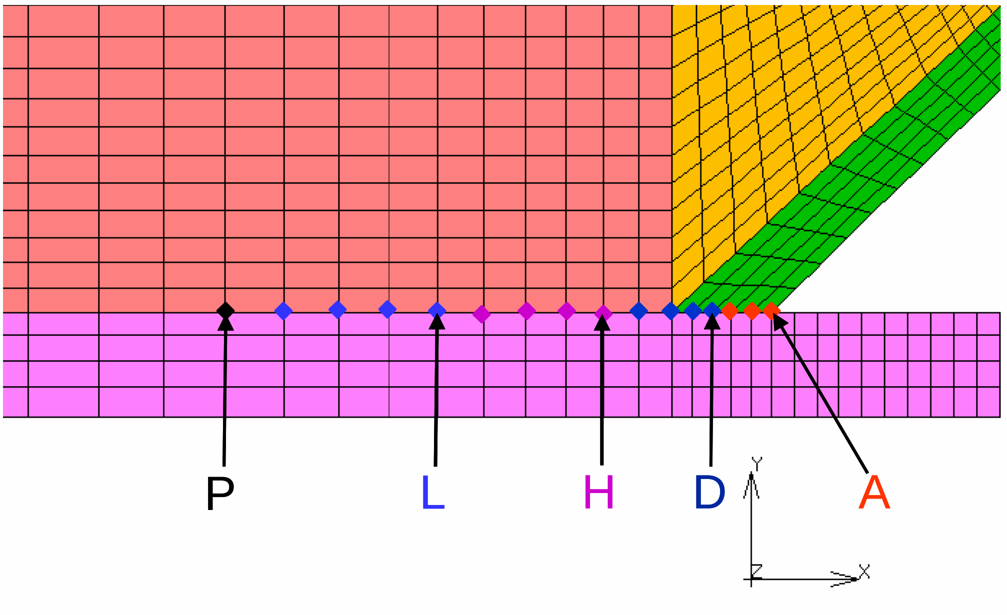

Nevertheless, the measured stress (outside of the core) on point A leads to stress variations of 375 MPa which are higher than those predicted for a cold shock from 510℃ to 105℃ (instead of 510℃ to 180℃ for experimental tests). For point C, the calculated stress is 308.3 MPa. In term of strain, the differences between simulations and experimental results may be more pronounced

- Moreover, even far away from the hot inlet (in the middle of the heat exchanger), the stress amplitude is quite similar to near the inlet one whereas simulations tend to show an important decrease when moving along different points defined on the previous picture.

4. CONCLUSION

Within the HTR-E program, some recuperators have to be tested on a test rig of the GREThE. The main aim of this work package 2 was to estimate the viability of different technologies. At the moment, only a PCHE technology has been tested.
Experimental tests were carried out on a mock up designed by HEATRIC. These tests were done on CLAIRE loop located at CEA research centre at GRENOBLE.
The tests were realized in steady and transient conditions. In steady conditions, it was intended to check the ability of this technology to reach HTR recuperator specifications in term of thermal duty and pressure loss.
In steady state, the following results are obtained:

- Hydraulic tests were carried out at ambient temperature leading to Heatric predictions (cf paragraph 2.1).
- Thermal tests were carried out at different temperature levels. A discrepancy between experimental results and Heatric predictions is noticed and explained.

  Indeed, from initial prediction given by HEATRIC at nominal point, the effectiveness was supposed to be around 97.6 %. Three main corrections could explain the experimental effectiveness equals to 95.3% (+/- 0.3 %):

  - An adjustment of air physical properties generates a decrease of effectiveness of 0.8 %
  - Adding an effect of longitudinal wall conduction leads to a decrease of effectiveness of 0.5 %
  - Assuming a flow mal distribution between plates can easily generate a loss of effectiveness around 1%.

  So by adding the three effects, the experimental effectiveness can be justified. **Moreover, it must be kept in mind that the heat exchanger fulfils the specification in the way that 95% effectiveness is reached as in GT-MHR specification.**
  The discrepancy can not be linked to an error on thermal law in corrugated channels since the experimental effectiveness should not increase when mass flow rates are increased.
  So to go further in these investigations, it would be worth modifying the inlet pipes to avoid (or decrease) a jet effect which seems to occur more especially on hot side since the inlet velocity is higher than one on cold side. **For GT-MHR application, HEATRIC did not propose the same alimentation of the channels and therefore no jet effect would occur at the inlet.**

In transient state, the HEATRIC heat exchanger was submitted to severe temperature variations (i.e. same ones than those of HTR recuperator). During the cold shock the temperature varied from 510℃ to 180℃ within five seconds. When temperatures inside the heat exchangers were quite stabilized, a hot shock from 180℃ to 510℃ within 3 minutes was applied. Strain gauges located outside of the core showed that high stresses were applied to heat exchanger more especially near the hot inlet: 375 MPa variations during a thermal shock. The thermo mechanical analysis tends to show a modification of the behaviour of the heat exchange with time: formation of local plastic area.

These 2 temperature variations were repeated 100 times without giving raise to internal leaks (checked with helium tests).

In conclusion, HEATRIC heat exchanger gives satisfying results under air tests and it should be submitted to helium tests in real working conditions to go further in the analysis. HEATRIC seems to be a potential candidate for providing reliable recuperators.

5. BIBLIOGRAPHY

1. HTR-E-Recuperator, specifications of typical operating conditions for HTR" by Framatome ANP, First issue, 31/05/2002.

2. M.M. Ali and S. Ramadhyani, Experiments on convective heat transfer in corrugated channels, Experimental Heat Transfer, vol. 5, pp. 175-193, 1992

3. P.G Kroger, Performance deterioration in high effectiveness heat exchangers due to axial heat effects, Advances in Cryogenic Engineering, Vol. 12, 363-372 (1967).

4. J.H.Fokkens & S.M.Willemsen, HTR-E WP2, Thermal and Mechanical Analyses for Heatric Mock-Up, 14/09/2005.

Annex 1: Test report in transient conditions written by French welding institute.

INSTITUT® DE SOUDURE	2455		MF1040P	5007F	2595	**PAGE** *SEITE*
	RAPPORT N° : *REPORT N°* *BERICHT-NR*		**RE-43252**			28 / 1
				date :	22/11/05	
	RDT-CAQ - 1006 - 99		PC-2611		Rév 0	

RAPPORT D'ESSAI

TEST REPORT - PRÜFBERICHT

Transmis à : **C.E.A**
Transmitted to
Übermittelt an

AUTEUR : **D. COLCHEN**
Author - *Autor*

VISA :
Visa - *Stempel*

RESPONSABLE D'ACTIVITÉ : **P. MONTHERAT**
(ou son délégué)
Section Leader (or representative)
der Verantwortliche (oder sein Vertreter)

VISA :
Visa-*Stempel*

le : **22/11/2005**
Data - *Datum*

TITRE : **Strain and displacement measurement on a heat exchanger**
Title - *Titel*

N°Cde à IS : **4000138630/P7N23 du 02/07/04**
Order to IS - *Bestellung Nr IS*

SUMMARY

PLATES

STRAIN AND DISPLACEMENT MEASUREMENT ON A HEAT EXCHANGER

INTRODUCTION

The Fatigue and Fracture Mechanic laboratory from Institut de Soudure realised instrumentation with strain gages and displacement captors on a heat exchanger for C.E.A. These tests were carried out within HTR-E program in the work package WP 2 “Recuperator”. The heat exchanger is a diffusion bonded heat exchanger provided by Heatric (UK).We also added a recorder in order to measure the strain during the different phases of heat and cooling. At least we defined the stresses as a function of equations given by C.E.A and also defined in RCC-MR(AFC85) .

EXPERIMENTAL CONDITIONS

The plate 1 shows the location of the different strain gages on the heat exchanger.

The type of gages 1 to 4 and 6 is the following: HEAT SL 050 P-H120, the type of the gage 5 is the following: KFU 5-20-17-6
Three displacement captors are set on the heat exchanger. Settings have been used in order to attach the displacement captors on the heat exchanger under the heat insulation. The positions of the captors are the following:
-One in the longitudinal direction of the heat exchanger
-One in the lateral direction on the hot side of heat exchanger
-One in the lateral direction on the cold side of heat exchanger.

The gages 1 to 4 and 6 are directly welded on the upper side of the heat exchanger; the last one is bonded with special hot setting glue. One thermocouple is brazed near each gage in order to define the real strains as a function of the level of temperature near the gage.
Plates 2 and 3 present few views of the gages, thermocouples and displacement captors.
All of the captors are connected on a dynamic recorder. The type of recorder used is a MGC+ from HBM.

The data records were made each work day by employees of the C.E.A. during all the time of the test on the heat exchanger.

RESULTS OF MEASURING

The data are very consequent; therefore all the results are presented on 3 compact disks.

These compact disks present the results in terms of strain variation associated with thermo couples and the displacement variation as a function of the time.
The compact disks present also the results in terms of stresses as a function of the time for the different strain gages.
The technique used in order to define the stresses is the following:

- in the case where the measured strains are lower than the elastic strain defined at a specific temperature, then the calculated stresses are equal to :

  $\sigma = \varepsilon_{measured} \text{ x } (194000\text{-}81.4\text{x}T)/10^6$

  (Equation given by RCC-MR (AFC85))

- in the case where the measured strains are greater than the elastic strain defined at a specific temperature, then the calculated stresses are equal to :

  $\sigma = \varepsilon_{elastic} \text{ x } (194000\text{-}81.4\text{x}T)/10^6 + 0.004622 \text{ x } (\varepsilon_{measured} - \varepsilon_{elastic})$

Where
T is the temperature measured with the thermocouples in °C
And

$\varepsilon_{elastic} = +/- (270.09 - 5.702*10^{-1} T + 9.1162*10^{-4} T^2 - 5.6188*10^{-7} T^3)*10^6 / (194000-81.4*T)$

Remarks :

The constant 0.004622 is the gradient of the plastic straight line; this value is defined by Prager model and issue from the tensile tests defined by the annex A3.15.6113a in the RCC-MR. Plate 15 presents the model of the tensile tests for different temperature.

I 'm supposing that the elastic strain is the same in tension or in compression, only the sign is different,

The different equations are accessible in the Excel plates.

The thought process in order to define the last equation is the following:

The measured strain is the sum of the elastic strain and the plastic strain, in the same way the total stress is the sum of the elastic stress and the plastic stress.

The elastic stress is obtained by the Hook law: $\sigma=\varepsilon * E$, which is the first term of the equation.

The second term of the equation is the equation of a straight line (the plastic straight line) with an offset equal to the elastic strain or stress in order to have a linear function.

RESULTS ANALYSIS

The results show following:

- The strain gages bonded symmetrically according to the longitudinal axis of the heat exchanger give the same strain evolution, nevertheless the difference of behaviour shown by the strains, for gage 6 the amplitude of strain is equal to 800 µm/m, for gage 4 the strain amplitude is equal to 1500 µm/m, but in terms of stresses the amplitude is quite equal between the both gages (see plates 4 and 5),
- The values of strain or stress (initial position of the stress or strain before hot and cold shocks) are not constant during the test, **this variation of the strain or stresses shows a modification of the behaviour of the heat exchanger** (see plates 9 and 10)
- The maximum and minimum values for gages 1, 2 and 3 are similar at the beginning and at half time of the fatigue test, nevertheless at the end of the test the maximum value of stress for gage 1 is 180 Mpa lower (see plates 8, 9 and 10),

- Gages 4 and 6 fluctuate conversely with gage 1,and the initial value of stress or strain at the beginning is increasing of a few Mpa , (50 Mpa for gage 4 and 10 Mpa for gage 6), in terms of strain these values are equal to 400 µm/m for gage 4 and 150 µm/m for gage 6,
- The same plates show the evolution of the stresses during the hot and cold shocks, in the first phase (cold shock) gages 1, 2 and 3 are in a compressive field (with similar values of maximum and minimum peak of stresses at the beginning of the test), gages 4 and 6 are in the same time in a tensile field, but gage 6 sees a increasing strain (or stress) rate more important than gage 4, in the second phase gages 1, 2, and 3 see a increasing strain (or stress) rate and show a uniform tensile stress field at the exchanger's enter, gage 4 an 6 see an important decreasing strain (or stress) rate and show a uniform compressive stress field in the middle of the heat exchanger. These behaviours are the same during all the fatigue test
- The displacement captors show very small variation of dilatation of the heat exchanger (few millimetres in the longitudinal axis and less than one millimetre for the both transversal captors (Nevertheless the attachments of the captors are not perfect so the recorded values are giving only a order of magnitude) see plate 11 .

In conclusion of these analysis, the results show an equilibrium of the heat exchanger, when gages 1, 2, 3 are decreasing in stress or in strain, the gages 4, and 6 are increasing in the same order, so for a contraction of the enter part of the heat exchanger, we can see an expansion of the middle part of the heat exchanger, and conversely. During the fatigue test, we can observe a variation of point zero of gage 1, in order to conserve equilibrium of global stress field, gage 4 is varying conversely. This variation **shows an important plasticity near gage 1**, and **may be the presence of a fatigue defect**. The dimension of this fatigue defect is not quantifiable with the measurements.

Last point, the level of stress is not the same between gages 4 and 6 (in particular for the cold shock), and the stress rate is also different, so we can observe a stress decreasing more important for gage 6 than for gage 4 during the cold shock. It may be possible that the position of the gages is not exactly the same from each side of the heat exchanger, so we could have some differences, nevertheless it would be interesting to know how the fluid goes through the heat exchanger.

A last remark, the differences between the gages is more pronounced when we compare the strains, in fact the values in stress are levelling out because the slope of the plastic straight line is very small (m = 0.004622).

RESULTS ASSOCIATED WITH FATIGUE DATA

In order to define a fatigue life of the heat exchanger, we need some results in low fatigue life.
A study presented in PVP-Vol 350, Fatigue and Fracture from 1997 (Volume 1 ASME 1997), detailed the results of low fatigue life of a stainless steel (SS304) at 600 ℃.
This study gives in particular an S-N diagram of SS-304 plates for notched and unnotched plate at 600℃. The plate 12 shows the SN diagram.

For an unnotched plate the fatigue life for a nominal stress of 375 Mpa (value obtained on the heat exchanger) is equal to 4000 cycles (red lines), and for a notched plate the fatigue life is estimated to 150 to a maximum of 350 cycles (green lines) as function of the Kt (stress concentration factor) value.

The stress concentration factor is equal to the local stress divided by the nominal stress applied on the structure in an elastic behaviour of the material. The number of cycles applied on the heat exchanger is about one hundred cycles. We can also see on the plate 13 a significant modification of the stress variation on gage 1 and 4 and a little increasing of the stress for gages 3.
This modification of the behaviour of the gages is the sign of an important plastic area and is may be the sign of a presence of a fatigue crack located in the inner portion of the heat exchanger near the LP admission.

The study presents also the modification of the peak and mean stresses as a function of the number of cycle applied on the specimens. The plate 14 shows this behaviour in the study. We have the same behaviour on the heat exchanger for gage 1, the plate 13 shows a decreasing of the amplitude strain as function of time (number of cycles), and in particular gages 1. The authors of the study explain that the **variation of the stress** (mean stress and stress amplitude) is **due to a local plastic and creep strain accumulation**.

Plates 1 to 15

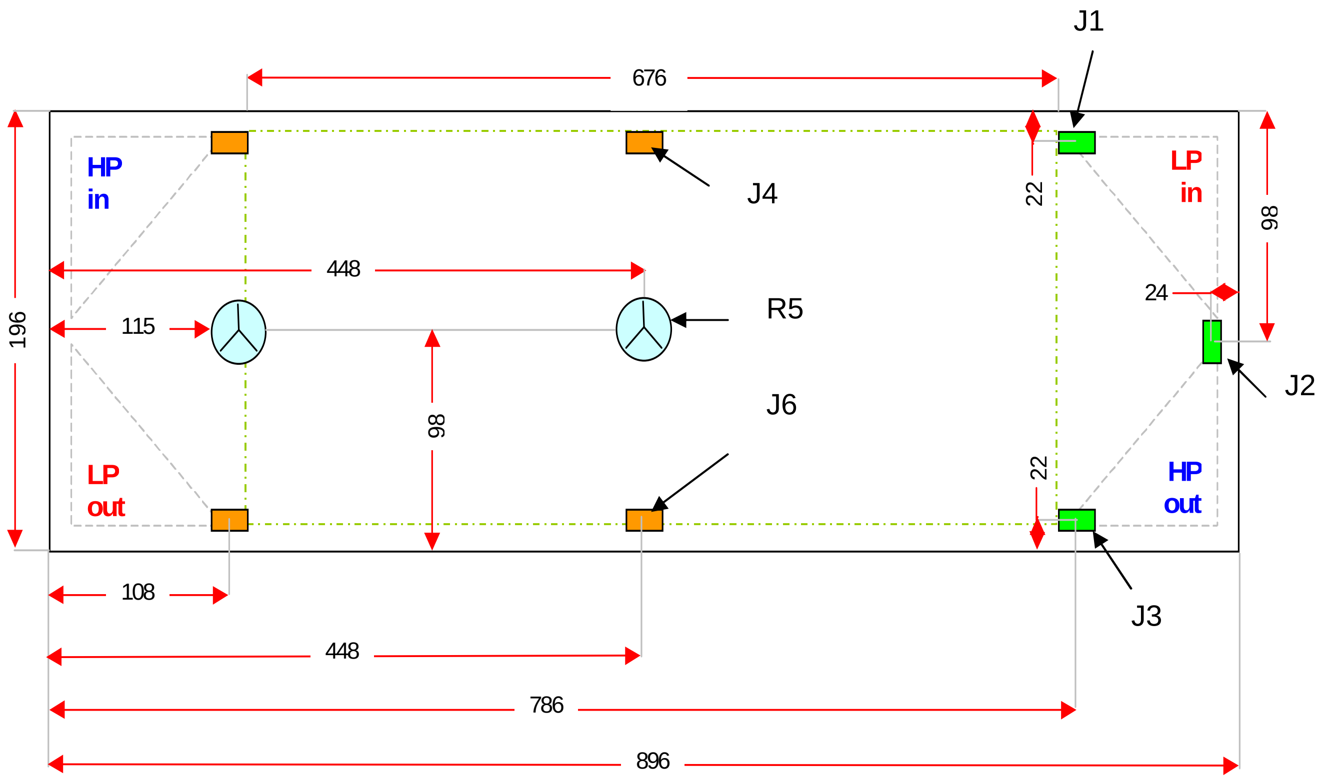

Plate 1: location of the gages and the thermocouples

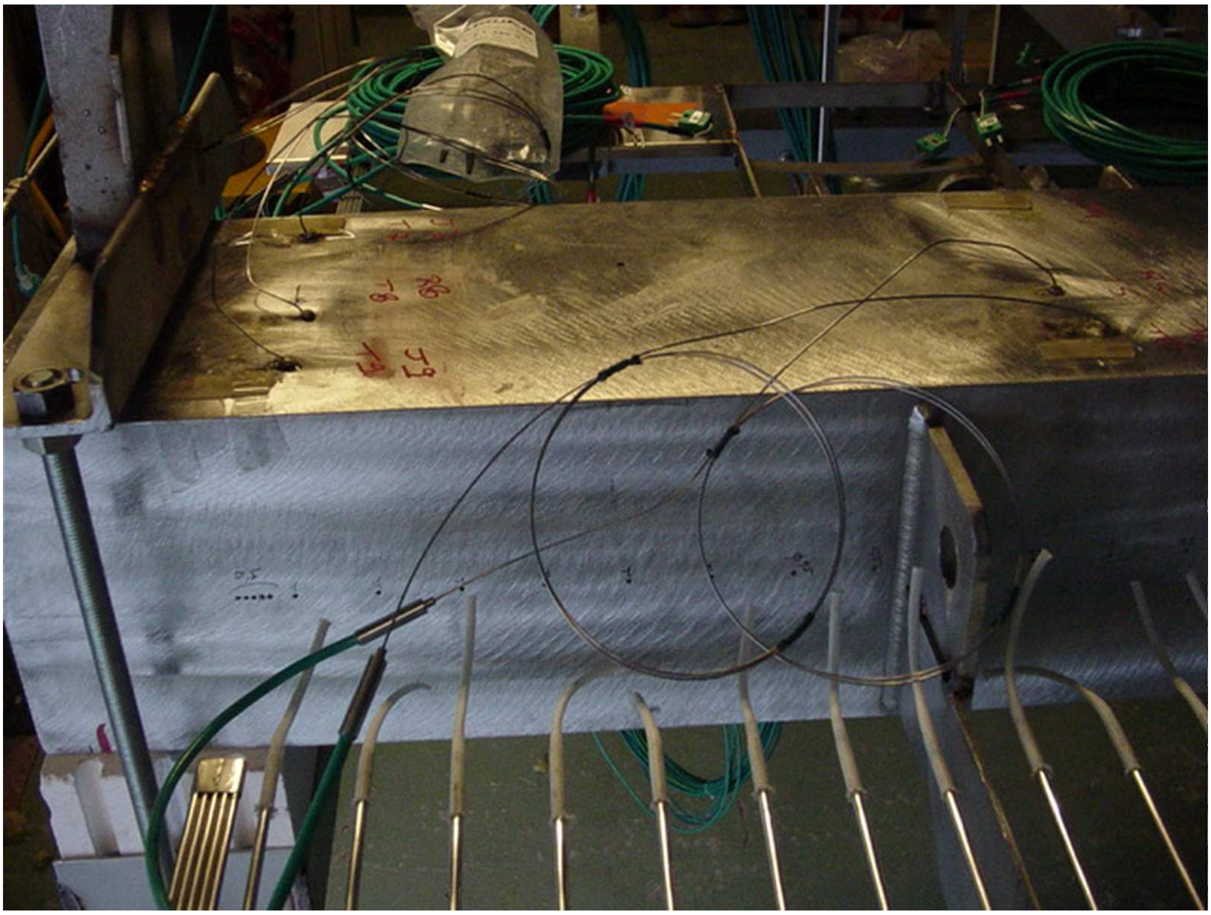

Plate 2: overview of the heat exchanger

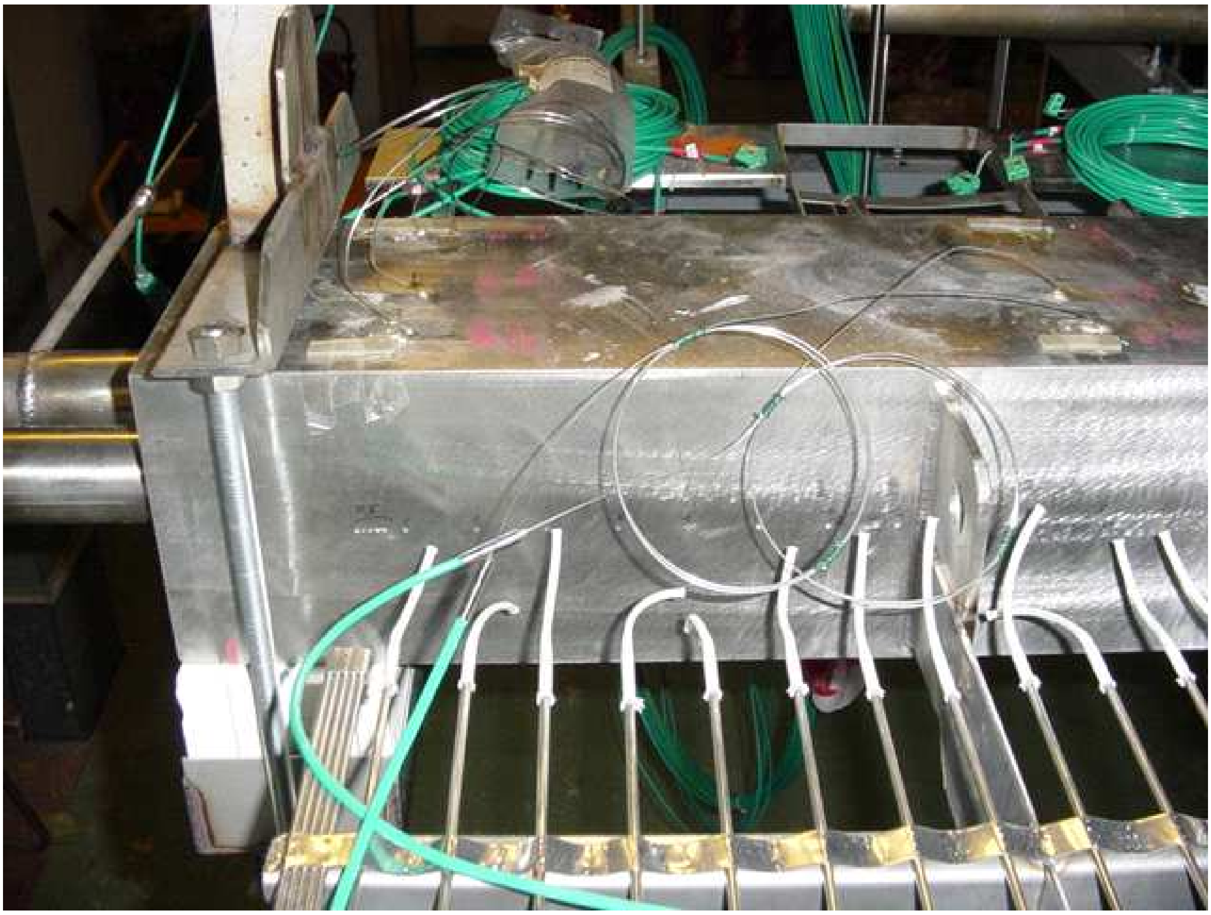

Plate 3: view of the gages 4, 6, and tri-directional gage 5, and the thermocouples

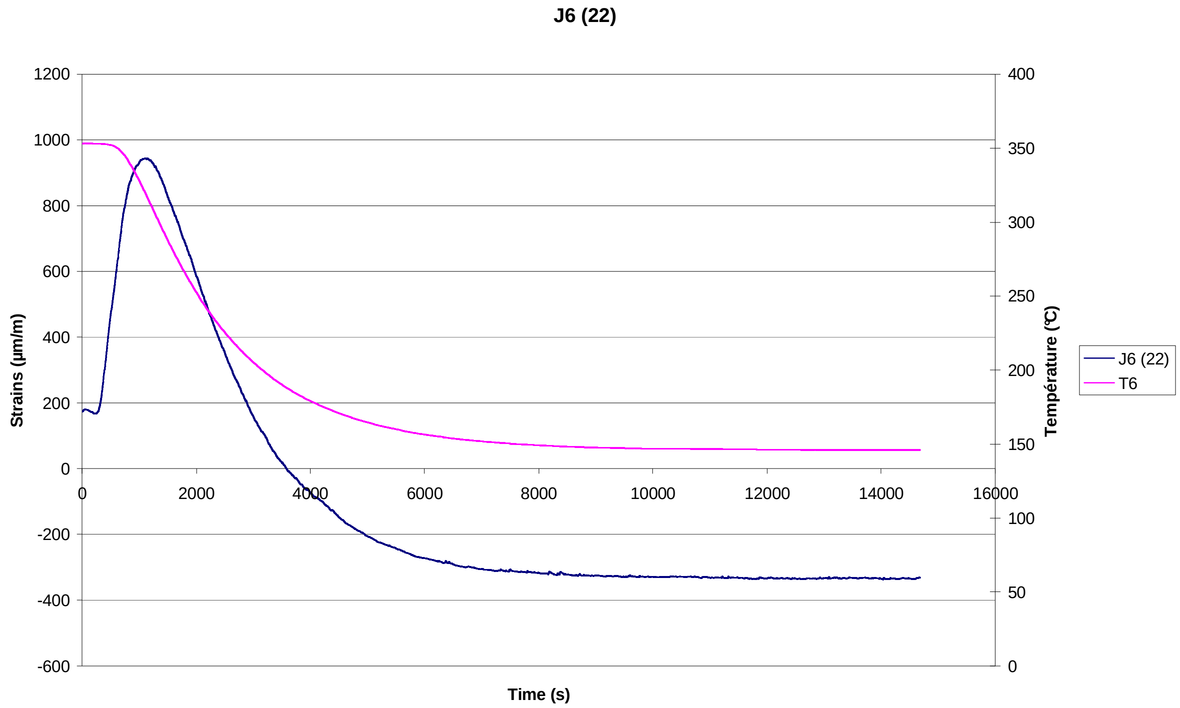

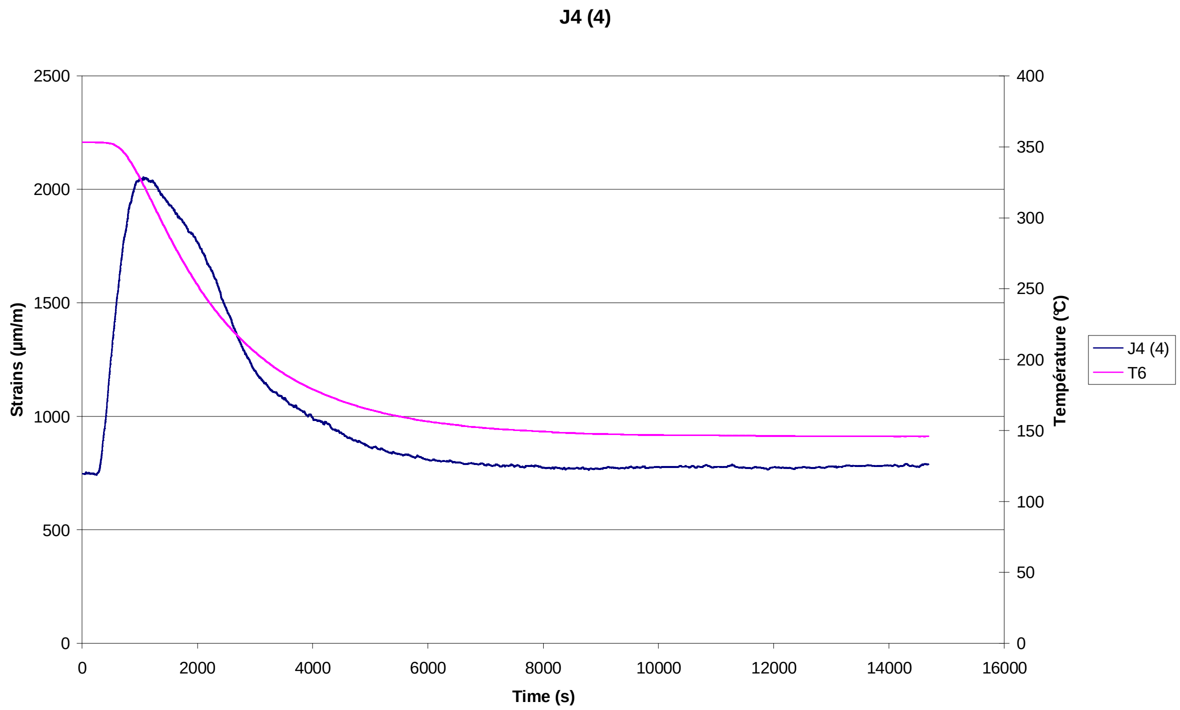

Plate 4: recorded values of gages 4 and 6 ; symmetrical response of the gages

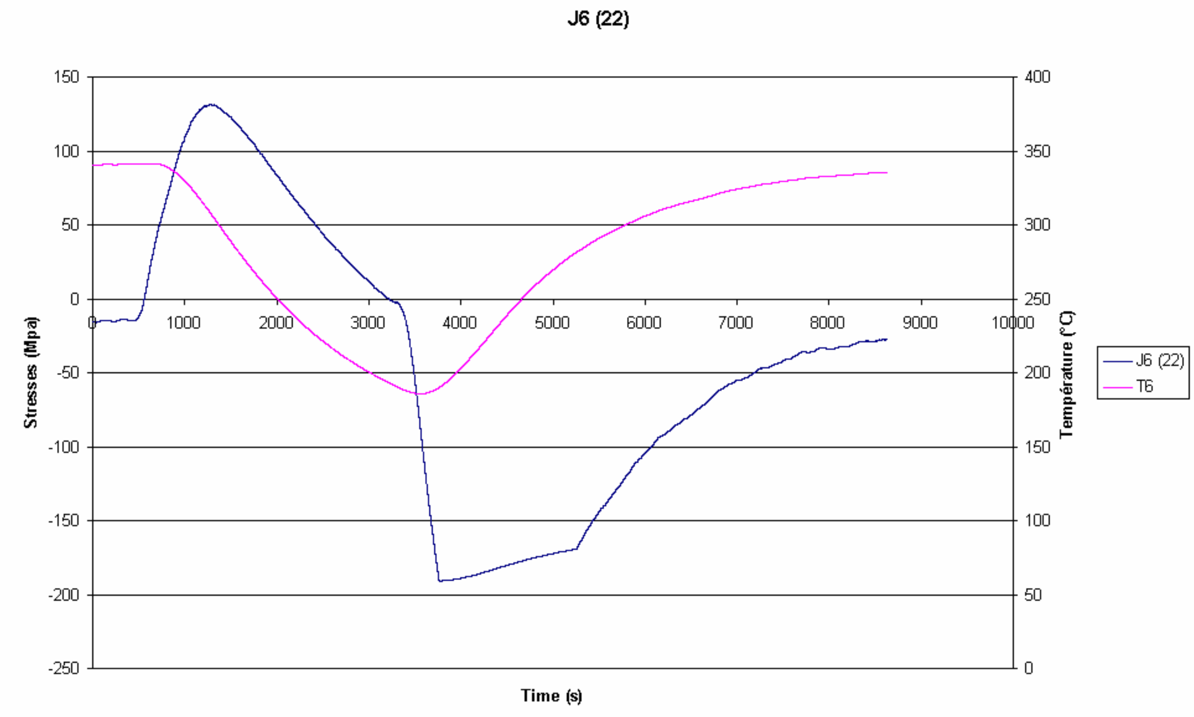

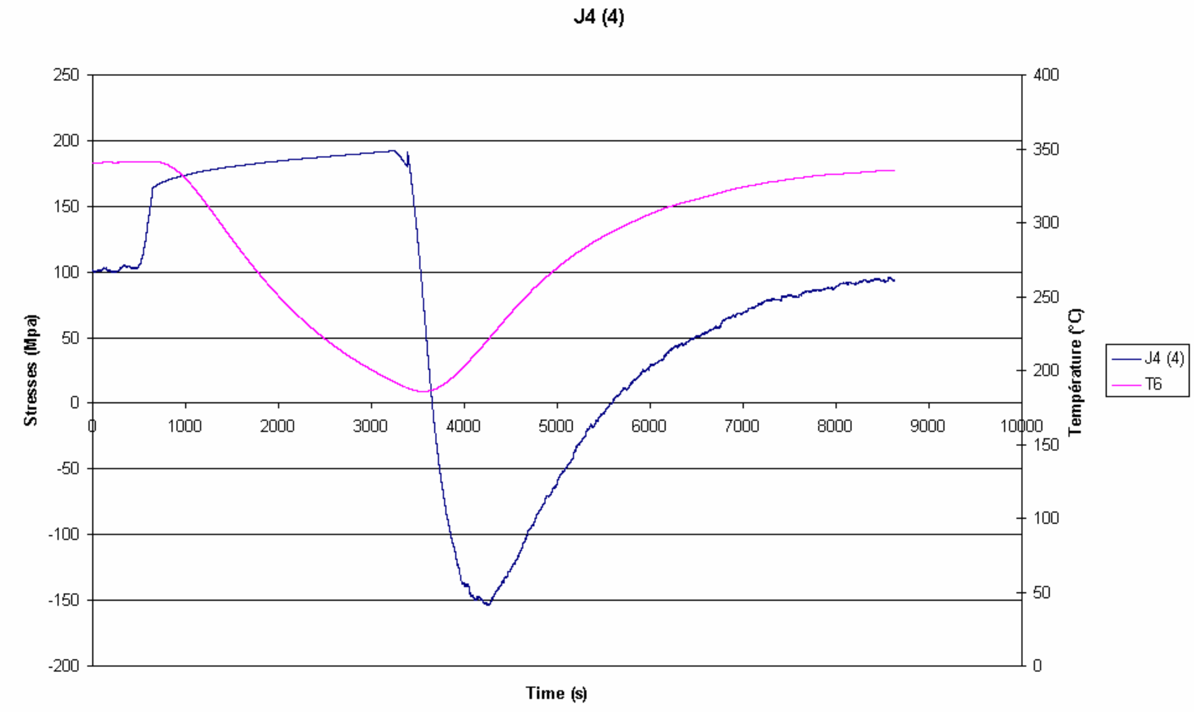

Plate 5: stresses variation values of gages 4 and 6; differences between the decreasing stress rate

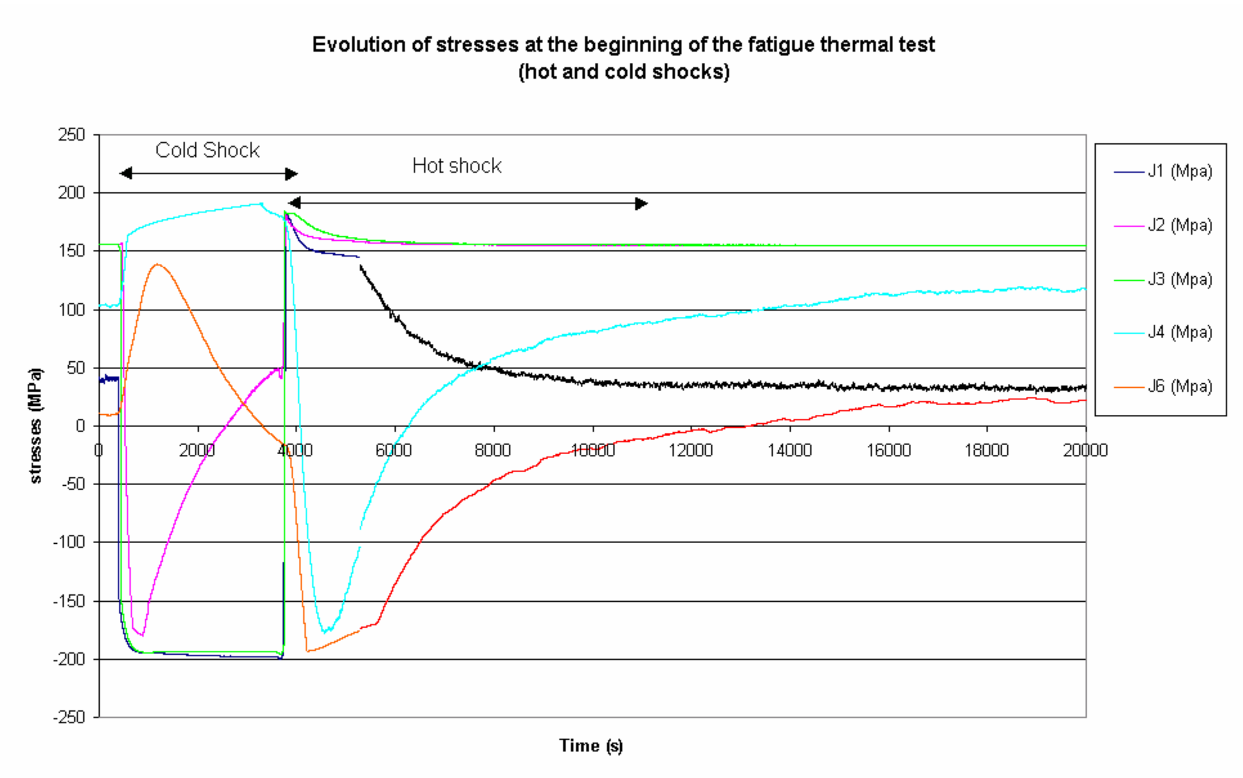

Plate 6: Evolution of the stresses at the beginning of the thermal fatigue test

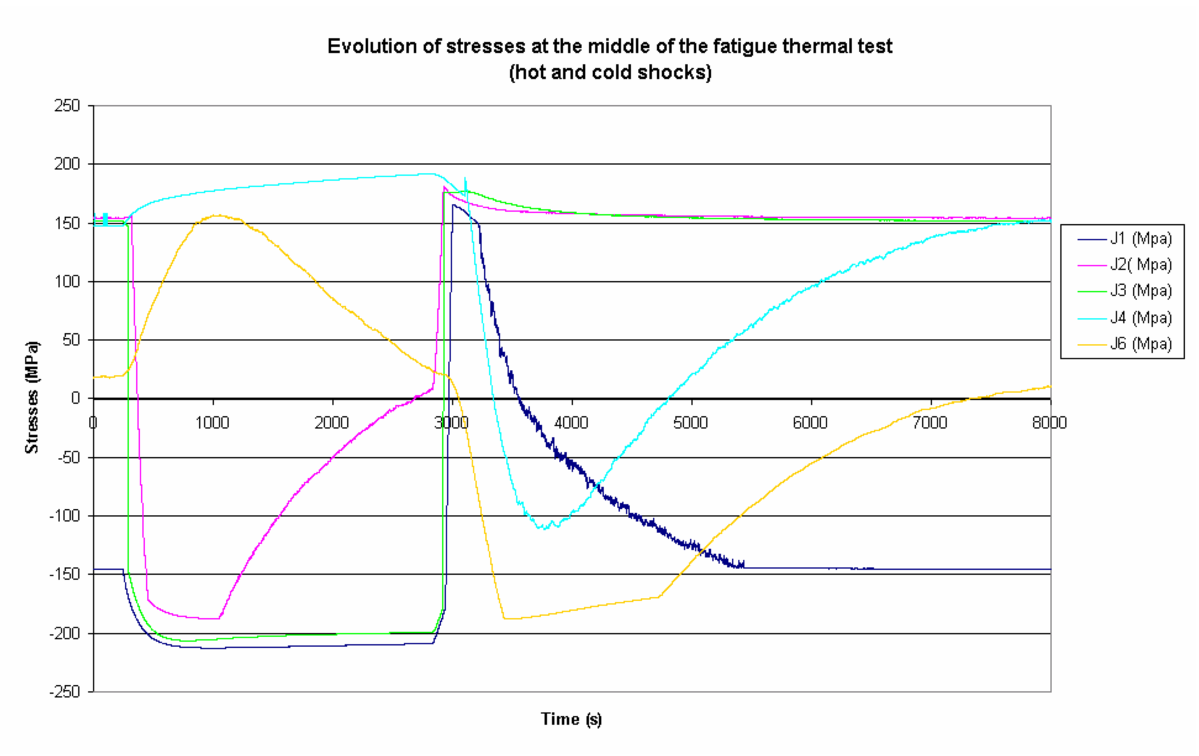

Plate 7: Evolution of the stresses at the middle of the fatigue thermal test

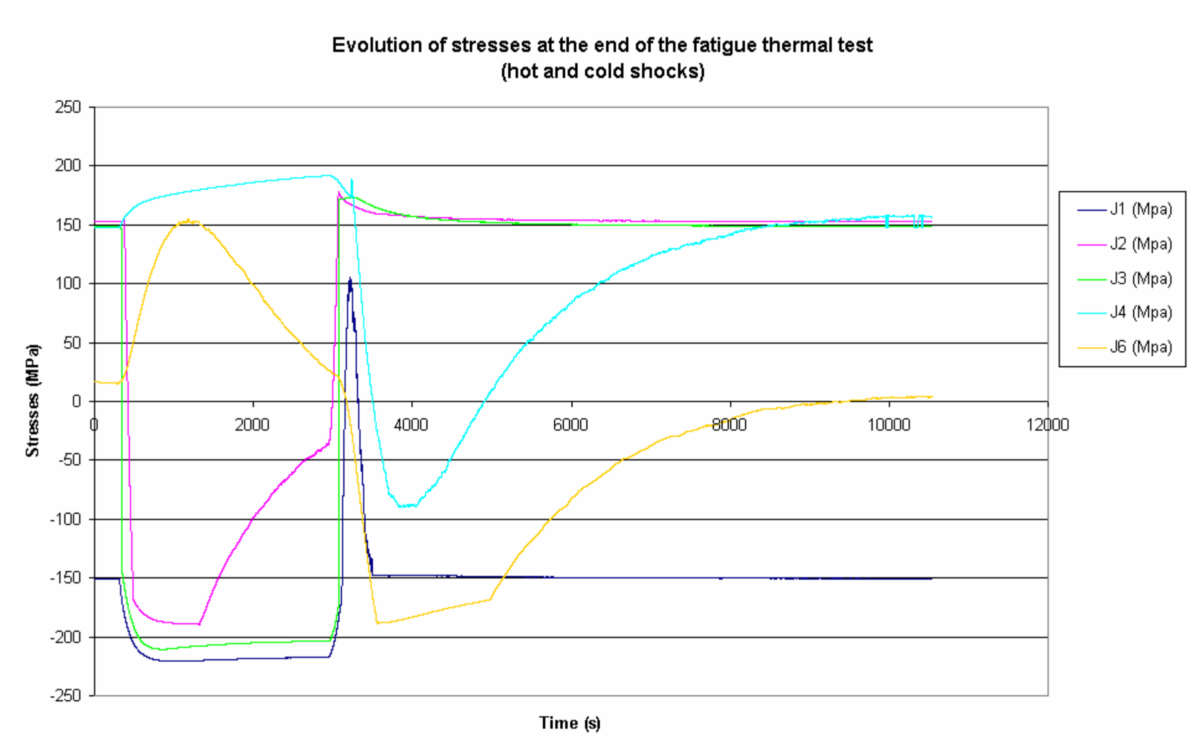

Plate 8: Evolution of stresses at the end of the fatigue thermal test

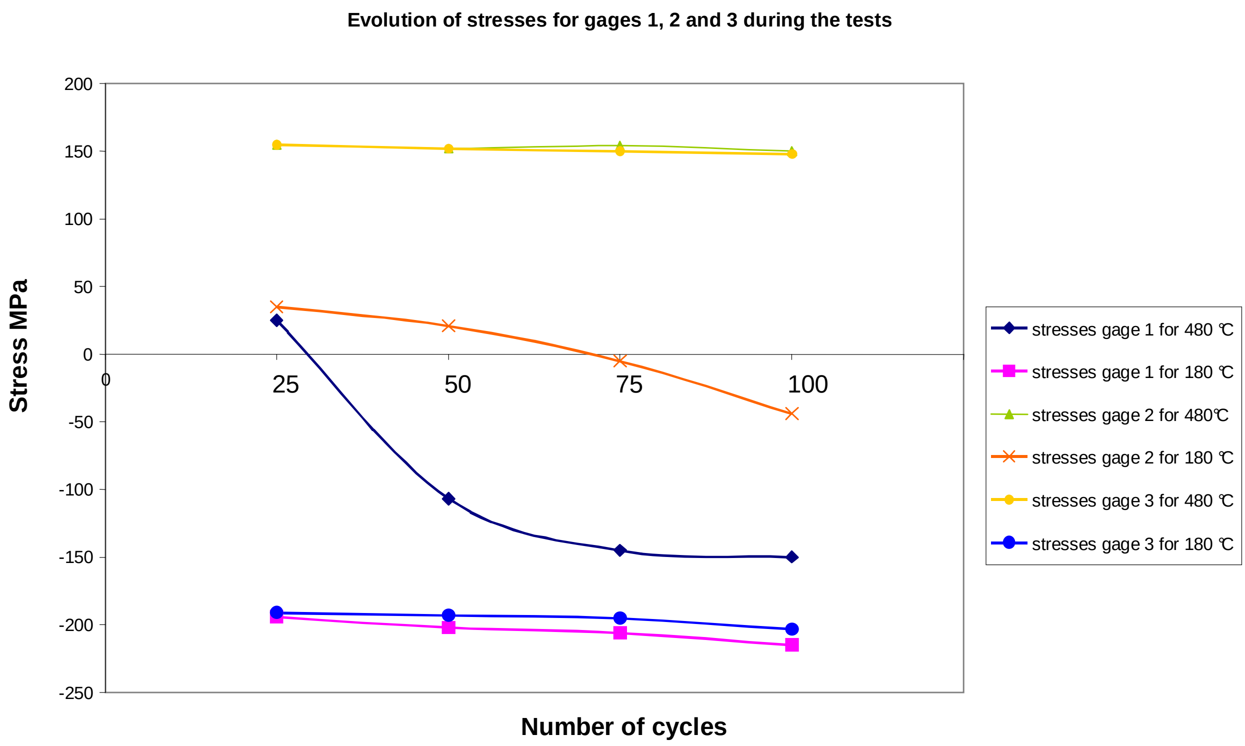

Plate 9: Variation of the stresses during the test on the heat exchanger

Evolution of strains for gages 1, 2 and 3 during the tests

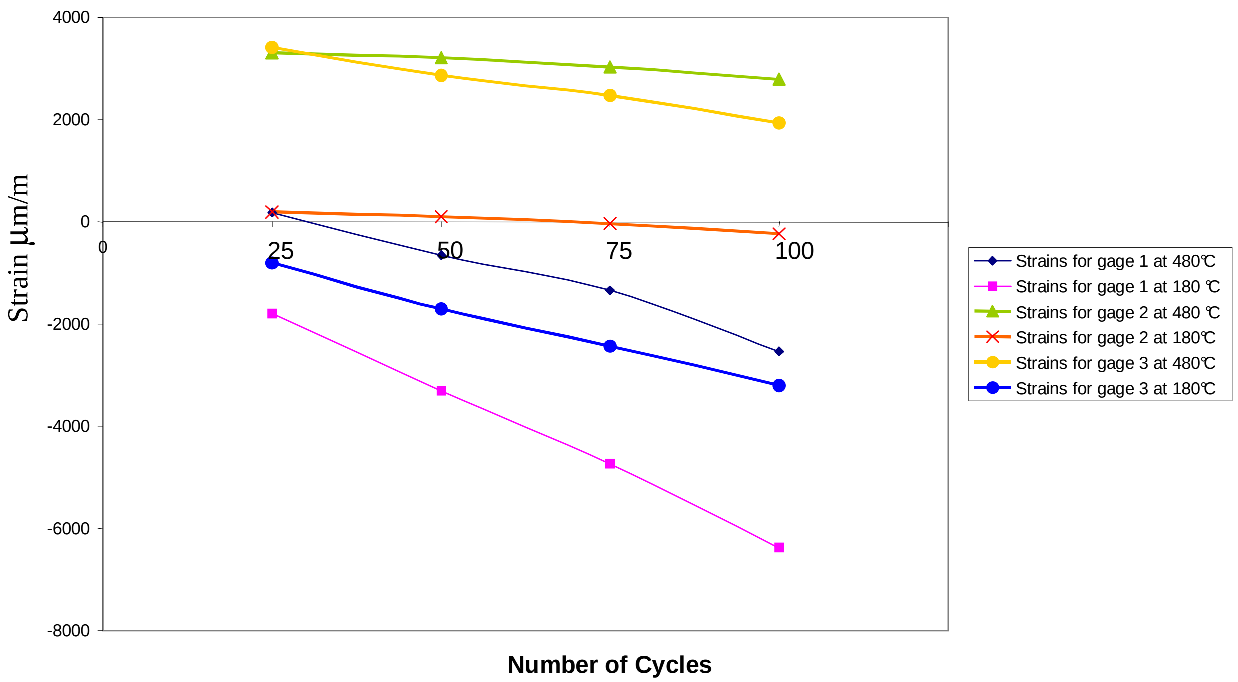

Plate 10: Variation of the strains during the test on the heat exchanger

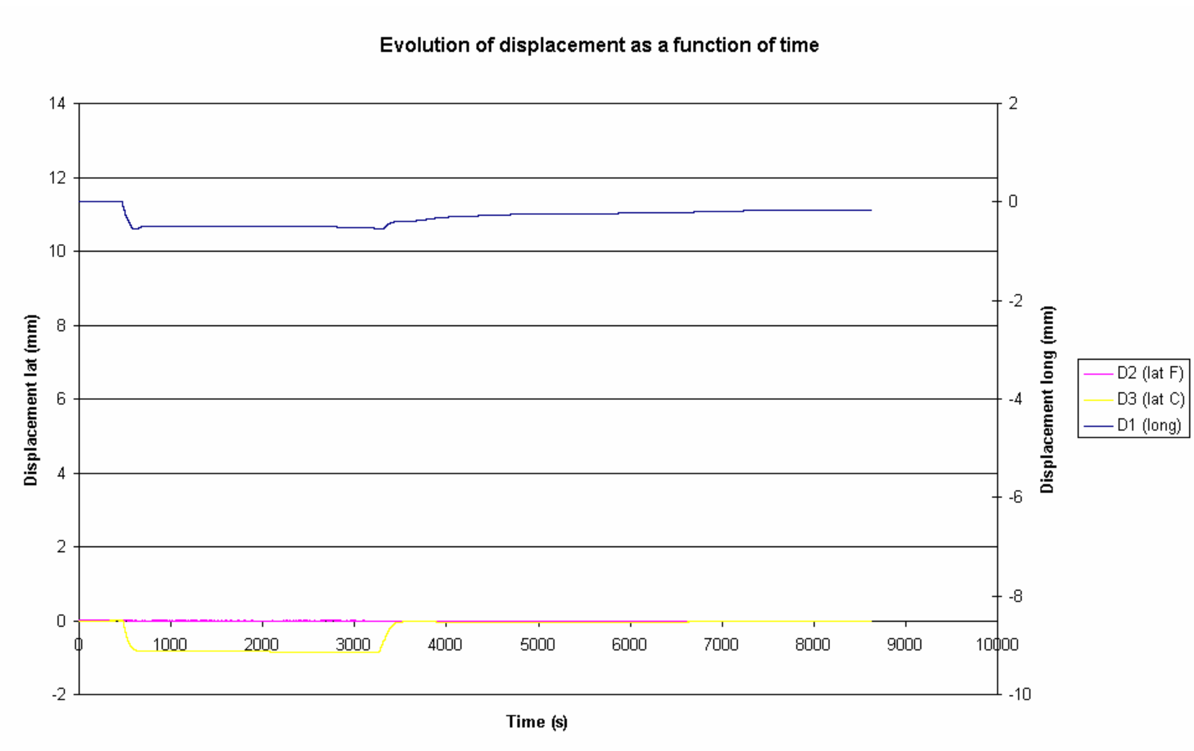

Plate 11: Evolution of the displacements at the middle of the fatigue thermal test

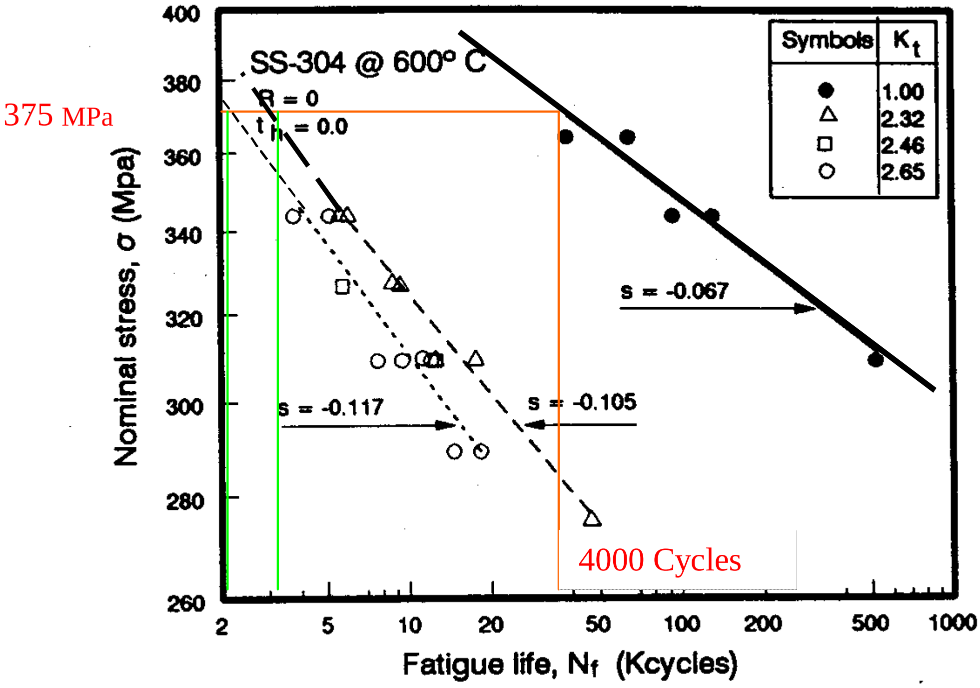

Fig. 2- σ-N_f curves for notched and unnotched plate specimens of SS-304 plates at 600° C

Plate 12: S-N curves from PVP Vol 350, Fatigue and Fracture 1997

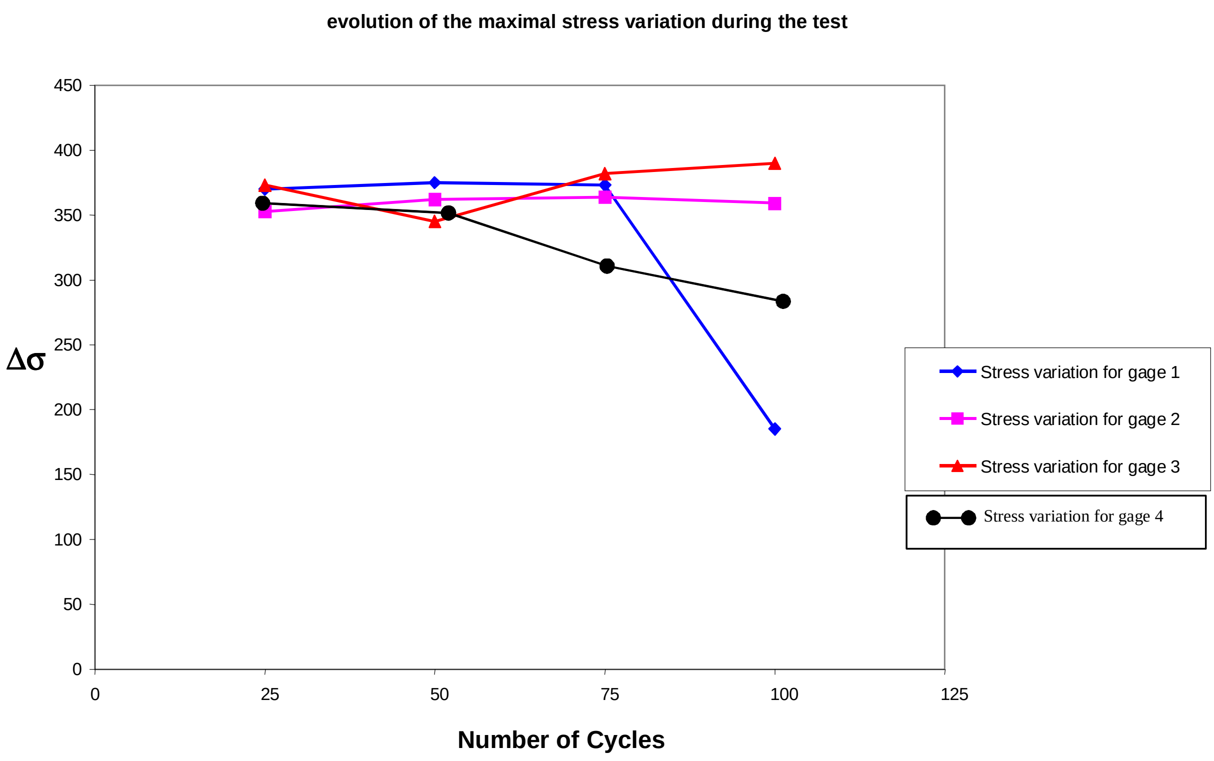

Plate 13: evolution of the stress amplitude during the test on the heat exchanger

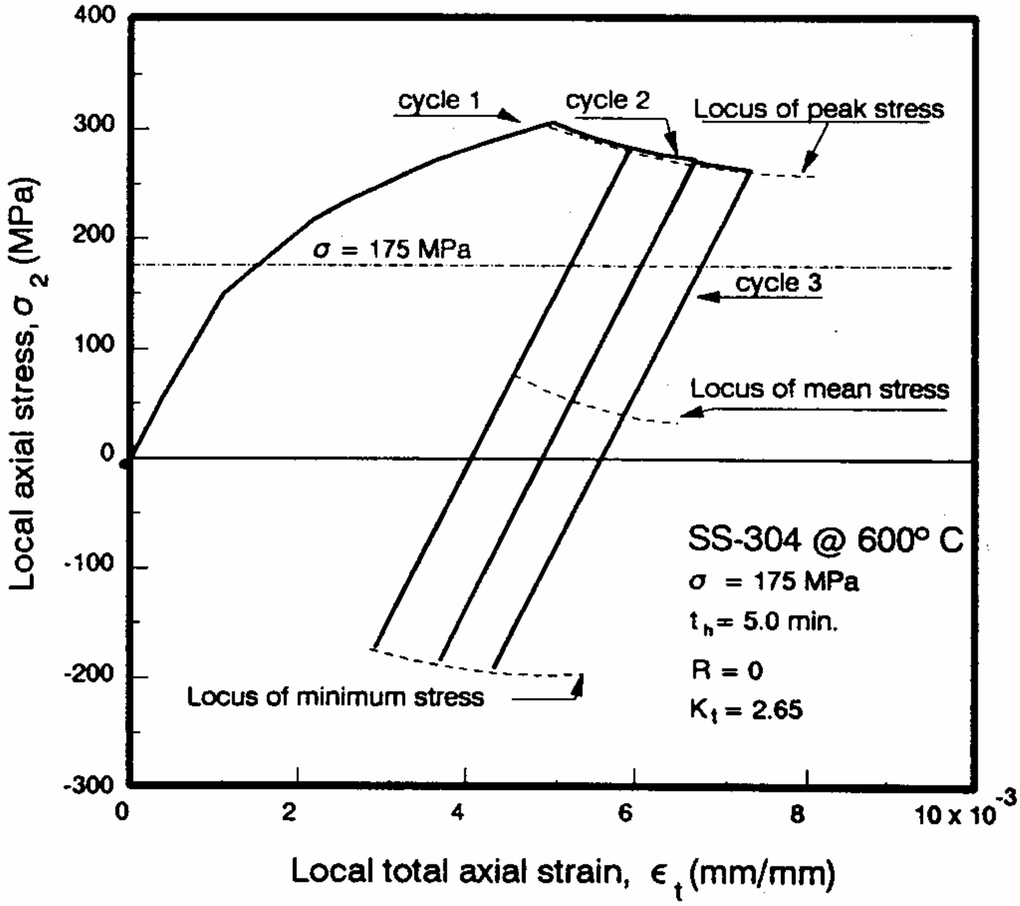

Fig. 12- Cyclic behaviour of local stresses in terms of local total strain

Plate 14: Cyclic behaviour of local stresses

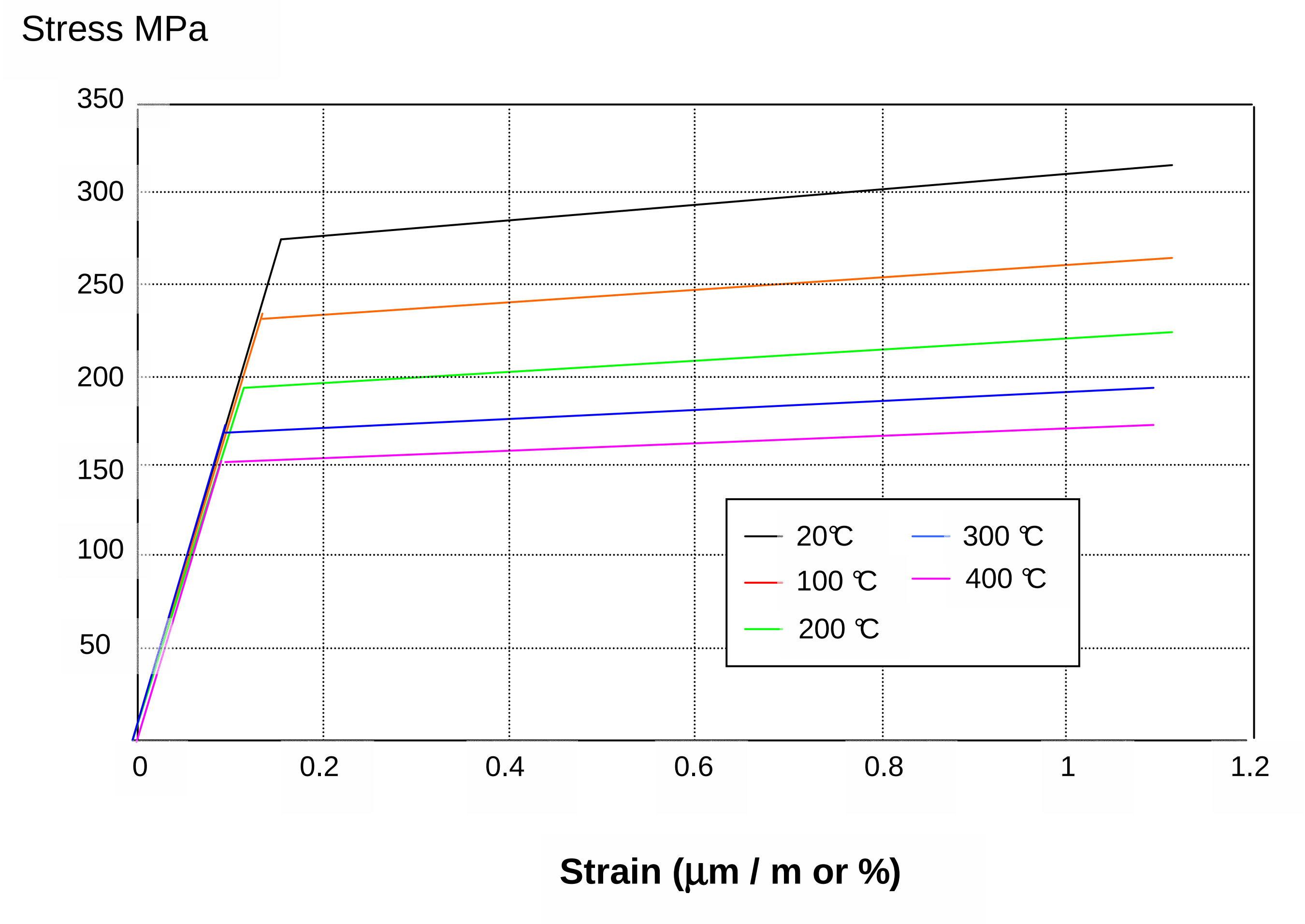

Plate 15 : Linear model of cinematic plastic law (PRAGER model) for a 316L stainless steel at different temperatures (Annex A3.15.6113a from RCC-MR)